 doi:10.20944/preprints202202.0113.v1

Article title: Delineating the tissue-mediated drought stress governed tuning of conserved miR408 and its targets in rice

Sonia Balyan, Shivani Kansal, Ringyao Jajo, Pratyush Rajiv Behere, Rishika Chatterjee and Saurabh Raghuvanshi*

All Author Affiliations:

Department of Plant Molecular Biology, University of Delhi South Campus

New Delhi 110021, India

***Corresponding author:**

Dr. Saurabh Raghuvanshi

Professor

Department of Plant Molecular Biology, University of Delhi South Campus

New Delhi 110021

Email: saurabh@genomeindia.org

Phone: +91 9811574152

Abstract

MicroRNAs act as the cardinal post-transcriptional monitors of gene regulatory networks sculpturing the developmental plasticity and stress responses in plants. Single miRNA target several genes and how the transcriptional regulation of miRNA impacts its pool of targets in different tissues and stress conditions is still elusive. The present study investigated the highly conserved and evolving MIR408 family comprehensively by redefining its evolutionary conservation and diversification in plants followed by detailed functional analysis in rice. MIR408 family comprises three dominant mature forms (21 nt) including a distinct monocot variant. Plant MIR408 family can be divided into six groups. miR408 majorly cleave genes belonging to blue copper protein in addition to several other species-specific targets in plants. Screening of 4726 rice accessions identified 22 sequence variants in 1 Kb upstream (15) and MIR408 region leading to the identification of 8 haplotypes (3: Japonica-specific and 5: Indica-specific). miR408-3p follows flag leaf preferential and drought upregulated expression profile in flag leaf and roots of N22 which seems to be regulated by differential fraction of mCs in the precursor region. The active pool of miR408 regulated targets under control and drought conditions is impacted by the tissue type. Comparative expression analysis of miR408/target module under different sets of conditions

 doi:10.20944/preprints202202.0113.v1

features 83 targets exhibiting antagonistic expression in rice. Twelve high confidence targets including 4 plantacyanins (OsUCL6, 7, 9 and 30), pirin, OsLPR1, OsCHUP1, OsDOF12, OsBGLU1, glycine rich cell wall, deoxyuridine 5-triphosphate nucleotidohydrolaseand OsERF7 with antagonistic expression under most conditions. Further, over-expression of osa-MIR408 in drought sensitive rice cultivar leads to the massive enhancement of vegetative growth in rice with improved ETR and Y(II) and enhanced the dehydration stress tolerance at seedling stage.

Keywords: miR408, conserved, drought, N22, miRNA target

Introduction

Global climatic fluctuations are the ultimate threat to the aim of achieving future food security for the constantly increasing population. Drought is one of the leading adversities accounting for global yield losses of major cereals, specifically rice. To bypass the hurdles, it's important to comprehensively delineate the complex multi- level molecular regulatory mechanism activated and functioning in response to drought stress especially in the wild tolerant cultivars. MicroRNAs (miRNAs) have recently emerged as the crucial key regulators of molecular stress responsive strategies. miRNAs are tiny (20-22nt) indispensable post-transcriptional regulators of core to sophisticated molecular gene circuits impacting growth, development and biotic as well as abiotic stress responses in plants. Differential regulation of several miRNAs in response to drought was reported by previous studies (Nadarajah and Kumar, 2019[1]; Kansal et al. 2015[2]; Singroha et al. 2021[3]). But only a handful of miRNA-target nodes were functionally characterized for their role in imparting drought stress tolerance in plants. miR394a/F-box gene module plays a critical role in conferring drought stress in *Arabidopsis* (Ni et al. 2012[4]). miR169o acts as a positive regulator of drought tolerance in poplar by regulating its target, NF-YA6 (Jiao et al. 2021[5]). In contrast, miR169n functions as a negative regulator of drought tolerance by targeting NF-YA8 in *Brassica napus* (Li et al. 2021[6]). Moreover, several other miRNA/target nodes are reported as the critical regulator of drought stress tolerance e.g., miR827/Rab17 in barley (Ferdous et al. 2017[7]); miR169/NF-YA in tomato (Zhang et al. 2011[8]) and miR166-OsHB4 in rice (Zhang et al. 2018[9]). Since their discovery, hundreds of MIRNA gene families have been annotated in several plant species, which was accelerated in the past few years with dynamic rate due to the advancement in next generation sequencing solutions. While several of the MIRNA families exhibited lineage or species-specific occurrence, most

 doi:10.20944/preprints202202.0113.v1

are conserved along the evolution of plants (Cuperus et al. 2011[10]). miRNAs bind to their target transcripts based on homology and lead to the cleavage or translational inhibition (Axtell et al. 2007[11]).

One such conserved miRNA family is *MIR408* (Kozomara and Griffiths-Jones, 2014[13]), which governs the growth, development and yield related traits through enhanced photosynthesis via regulating its conserved target gene family *PLANTACYANINS* (Zhang et al. 2018[14], Pan et al. 2018[15]; Zhang et al. 2017[16]; Zhang et al. 2013[17]). miR408 is a critical node in the copper economy mode conserved in different plant species (Zhang et al. 2013[17], Yamasaki et al., 2007[18]). In rice, miR408-UCL8 module is implicated in the control of grain yield and photosynthesis (Zhang et al. 2017[16]). Recently, PIF1-mediated direct transcriptional repression of *MIR408* modulated the post-transcriptional regulation of blue copper protein, *PLANTACYANIN* (*PCY*) during the early germination in *Arabidopsis* (Jiang et al. 2021[19]). In response to copper and light, *SPL7* and *HY5* coordinate the transcriptional activation of *MIR408* resulting in repression of targets to allocate copper to plastocyanin (Zhang et al. 2014[20]). MIR408 overexpression in *Arabidopsis*, rice and tobacco showed increased chloroplastic copper, plastocyanin abundance and photosynthesis in addition to higher rates of vegetative growth and enhanced seed size and weight (Pan et al. 2018[15]; Song et al. 2018[21]). Further, miR408-TaTOC$_{1s}$ is involved in regulation of heading time in wheat (Zhao et al. 2016[22]). *MIR408*-mediated enhanced biomass and yield traits were primarily due to cell expansion (Song et al 2018[21]). Besides being the conserved positive regulator of plant growth and development, miR408 also reported to be modulated in response to several environmental cues. MIR408 overexpressing cowpea lines displayed enhanced drought and salinity tolerance (Mishra et al. 2021[23]). Further the improved drought tolerance due to overexpression of MIR408 was also reported in ryegrass (Hang et al. 2021[24]), chickpea (Hajyzadeh et al. 2015[25]). In addition, the *MIR408* overexpression leads to enhanced heat stress tolerance in ryegrass (Taier et al. 2021[26]). miR408-LAC19/25 was involved in the enhancement of saccharification efficiency, vascular development and lignification in poplar (Guo et al. 2021[27]). Previously, our group demonstrated the cultivar-specific drought stress-mediated response of miR408 in rice where its levels were upregulated in the flag leaf of tolerant cultivar but reduced in sensitive cultivar (Balyan et al. 2017[28]; Mutum et al. 2013[29]). In rice, the predominant targets of miR408 are several members of the plantacyanin family (Mutum et al. 2013[29]). In addition, several other genes from diverse families are also reported as targets of miR408 as evidenced from prediction as well as PARE data analysis. But in rice only few targets were discussed in

 doi:10.20944/preprints202202.0113.v1

detail. Further how the spatiotemporal and environment-specific abundance and regulation of miR408 could tailor the cleavage and abundance of its target transcripts still needs to be clarified. In addition, besides having few reports on miR408-mediated drought tolerance in plants, the direct evidence of it in rice is still lacking. We address the above question by taking miR408, an evolutionarily conserved, tissue/-cultivar-specific drought stress regulated plant miRNA as a case study. Here in the present study, we map the detailed conservation and diversification of *MIR408* and its targets in plants. Complementing the miR408 levels with RNA-seq profiles of putative targets in flag leaf, inflorescence and root of control and drought stressed conditions of N22 rice. Considering the drought-regulated tolerant cultivar specific upregulation of miR408, here the overexpression MIR408 constructs were generated in drought sensitive rice cultivar, Pusa Basmati 1. MIR408-OE leads to the massive enhancement of vegetative growth in rice with improved ETR and Y(II). Further MIR408-OE PB1 lines perform better than WT suggesting miR408 as a positive regulator of growth, vigor and dehydration response in rice. Therefore, miR408 could be an important regulator for engineering and achieving the crops with enhanced vigor, yield and drought tolerance.

Material and methods

Plant material and stress conditions

Oryza sativa L. cv Nagina 22 (N22) was grown in the field and subjected to drought stress, 10 days prior to the expected heading stage of development. Stress was monitored by routine inspection of moisture content and leaf rolling phenotype. Flag leaf, panicle and roots from control as well as stressed plants were immediately frozen in liquid N2 and stored in -80 °C until use.

The wild type (WT) Pusa Basmati 1 (PB1) and PB1-MIR408-OE seeds were sterilized with 70% ethanol and then with 0.1% $HgCl_2$ having few drops of tween 20 with shaking for 15 min. Then washed with RO water several times and soaked in RO water overnight in the dark. Next day the seeds were spread on a cotton bed in small plastic trays evenly moisten with RO water. Trays were covered with a clean film and allowed to grow at 28°C ±2 in culture room conditions with a photocycle of 14 h light and 10 h dark for one week. Rice growth medium (RGM) were given as and when required. Two months old wild type and MIR408-OE plants were given dehydration stress (20% PEG in RGM solution) in tubes for 1 and 7 h followed by 2 days of recovery.

Multiple Sequence alignment and phylogenetic analysis of MIR408 family

Preprints (www.preprints.org) | NOT PEER-REVIEWED | Posted: 8 February 2022 doi:10.20944/preprints202202.0113.v1

The precursor *MIR408* and miR408 mature sequences from plant species belonging to different families were extracted from PmiREN2.0 (Plant miRNA Encyclopedia; https://www.pmiren.com). Multiple sequence alignment followed by phylogenetic tree construction of precursor miR408 was performed using the alignment tool of CLC genomics. The evolutionary tree was constructed using the Maximum likelihood method and Tamura-Nel model (Tamura et al. 2021[30]).

miR408 target identification and their conservation analysis

Degradome identified targets of miR408-3p were extracted from PmiREN2.0 (Plant miRNA Encyclopedia; https://www.pmiren.com; Guo et al. 2021[31]). Targets belonging to category ≤ 2 and cleavage evidence from ≥ 1 degradome library were considered. For studying the conservation of targets of miR408 in plants, the degradome identified targets from different plant species were extracted from PmiREN2.0. The degradome analyzed targets were used to extract their CDNAs from Phytozome followed by the phylogenetic analysis. The miR408 target genes from 16 different species with degradome evidence were used for conservation analysis. Phylogenetic tree was built using the NGPhylogeny.fr (https://ngphylogeny.fr) tool following the PhyML 3.0 (Guindon et al. 2010[32]) workflow. The tree was converted into a circular format and visualized using the MEGA11 software (Tamura[30] et al. 2021).

miRNA and mRNA expression analysis

The total RNA was extracted using TRI-reagent (Sigma-Aldrich) followed by DNAse I treatment (Thermo Scientific) as per instructions. The high-quality total RNA was used to enrich the small RNA using equal volumes of 4M LiCl followed by polyadenylation using Poly(A) Tailing kit (Ambion). 2 µg of polyadenylated small RNA and total RNA was reverse transcribed using miR_oligodT_RTQ (Ro et al. 2006[33]) and oligodT respectively followed by cDNA synthesis using SuperScript II Reverse Transcriptase (Invitrogen). To analyze the expression of miRNAs, the qRT-PCR was performed using Taqman Fast Universal PCR master mix (Applied Biosystems) with miR408 specific forward primer, fluorogenic probe specific to miR_oligodT_RTQ and RTQ universal reverse primer in Rotor Gene Q (Qiagene). For coding gene expression and MIR408, Fast SYBR Green master mix was used with gene specific primers. 5S and actin were used as endogenous control for miRNA and mRNA

Preprints (www.preprints.org) | NOT PEER-REVIEWED | Posted: 8 February 2022 doi:10.20944/preprints202202.0113.v1

expression respectively. ΔΔCt method was followed to calculate relative fold change ($2^{-\Delta\Delta Ct}$) in expression.

Gene ontology analysis and pathway analysis

The Gene ontology (GO) enrichment analysis was executed using the ShinyGO tool (v 0.741 http://bioinformatics.sdstate.edu/go/; Ge et al. 2021[34]) following P-value cutoff (FDR) as ≤0.05.

RNA-Seq profiles of miR408 targets

The expression of miR408 targets were extracted from the flag leaf, inflorescence and root of N22 under control as well as drought as conditions from Gour et al. 2021[35]. Transcriptome data of wild type and MIR408 transgenic seedlings were obtained from NCBI-SRA (Accession no. PRJNA412295; Zhang et al. 2018[14]). The raw RNA-seq files were analyzed using the RNA seq tool of CLC genomics workbench to obtain the RPKM values of genes.

Determining methylated cytosines

Methylation level in different tissues under control and drought conditions were determined by analyzing the whole genome bisulphite datasets using the bisulphite sequencing plugin of CLC Genomics Workbench (v9.0.1) following default parameters. Briefly describing, in order to call methylated cytosines, we deployed bidirectional protocol to map to the reference genome. The mapped reads were used as input for calling methylation level based on Fisher exact test (*p-value ≤0.05*) after removing non-specific matches, duplicate matches, and broken pairs reads. The error rate was determined by aligning reads to rice chloroplast and found to be ~1.44% in both control and drought stress samples. After incorporating the error rate, binomial distribution was calculated and the methylated cytosines were filtered based on *p*-value ≤ 0.005 with at least 5 reads in both the replicates. The methylated cytosines passing all these criteria were used for further analyses. Transcript information from RGAP (Rice Genome Annotation Project; V7.0; http://rice.uga.edu) was used to annotate the methylated sites through R Bioconductor packages of GenomicFeatures (v 1.46.1; Lawrence et al. 2013[36]) and ChIPSeeker (v1.30; Yu et al. 2015[37]). All the analyses were performed using custom R scripts built in-house. All the relevant information regarding methylated cytosines in the promoter and precursor region was extracted for flag leaf, roots and inflorescence under drought conditions.

Preprints (www.preprints.org) | NOT PEER-REVIEWED | Posted: 8 February 2022 doi:10.20944/preprints202202.0113.v1

Cloning of MIR408 precursor into binary vector and plant transformation

To generate Ubi::MIR408 construct, the 213bp (Chr1:12301661-12301873 [+]) pre-miR408 was PCR amplified using phusion (Thermo) Taq Polymerase from genomic DNA isolated from N22 seedlings using 5'- AGCGGTACCGGGAGTTCTGTGATTGG-3' and 5'-AGAGCTCACAGAGAGAGAGAGAGAG-3' primers. The PCR product was cloned into the pB4NU overexpression binary vector between the *Kpn*I and *Sac*I restriction sites. The construct was cloned in *E. coli* and confirmed by digestion and sequencing and then mobilized into *Agrobacteruim* for plant transformation. The transgenic rice plants overexpressing MIR408 under drought sensitive PB1 background were generated as per the protocol (Toki et al. 2006[38]).

Morphometric analysis of the over-expression transgenic

The transgenic lines were analyzed for their morphometric differences to the wild type plants. The shoot length, root length, root density, 3rd leaf length and width (from the midpoint) and whole seedling weight at different seedling stages were recorded for both transgenic lines and wild type plants. For most of the lines more than 10 plants were analyzed for each parameter. Measurements of relative water contents were determined as described previously (Dansana et al. 2014[39]). 5 cm of leaf segments were cut with the help of scissors and weighed immediately to determine the fresh weight. Then the segments were submerged in water for overnight period and their turgor weight was recorded. To determine the dry weight the segments were dried in the oven for 24 h and weighed. The RWC was calculated using the following equation: [(FW-DW)/(TW-DW)] x100.

Identification of variation, haplotype evaluation in 4726 rice accessions

The variations (SNPs and Indels) in the *MIR408* precursor and its 1kb upstream regulatory regions were detected in 4726 accessions using the 'variations by region tool' of RiceVarMap v2.0 (http://ricevarmap.ncpgr.cn; Zhao et al. 2021[40]). The variation IDs were then used as an input haplotype analysis using the 'Haplotype Network analysis' tool of RiceVarMap2. Further the chromatin accessibility map was generated using the 'Prioritization of regulatory variants by deep CNNs.

Results

Preprints (www.preprints.org) | NOT PEER-REVIEWED | Posted: 8 February 2022 doi:10.20944/preprints202202.0113.v1

Conservation and diversification of MIR408 across plant kingdom

With the advancement and ease in the accessibility of small RNA sequencing technologies, we have witnessed a surge in the identification and annotation of large repertoire of miRNA families in diverse plant species. More recently several comprehensive databases like PmiREN (Plant miRNA Encyclopedia; https://pmiren.com; Guo et al. 2020[31]) and sRNAanno (http://www.plantsrnas.org; Chen et al. 2021[41]) in addition to miRbase (the microRNA database; https://www.mirbase.org; Kozomara et al. 2019[42]) cataloged miRNA discovery, annotation and functional analysis in diverse plant species. This has enabled comparative genomics to explore the evolution of miRNAs across diverse groups of plant lineage. *MIR408* is one of the most conserved regulators of plant growth, development and stress response (Zhang et al. 2017[16], Pan et al. 2018[15]; Zhang et al. 2018[14]; Zhang et al. 2013[43]; Balyan et al. 2017[28]). But in the past decade, due to the limited coverage of miRNA annotation of plant kingdom, details of its evolutionary conservation and divergence across diverse plant lineages remained incomprehensible. Therefore, to extensively track the sequence diversity and conservation of MIR408 in plant kingdom, we have extracted the mature (miR408) and precursor (*MIR408*) sequences from 97 plant species annotated in PmiREN database covering bryophytes, spermatophytes, lycophytes, magnoliophytes including liliopsida and dicotyledons (Figure S1a). *MIR408* was not annotated in green algae in any of the databases. In the majority of the plant species (n=63), MIR408 family comprises a single precursor (Figure 1a). However, several plant species do show expansion of the MIR408 family and exhibited 2 (18 species), 3 (9 species), 4 (6 species) and 6 (1 species) precursors (Figure 1a). Highest number of MIR408 family members i.e., six precursors (MIR408a-f) were annotated in wheat (Figure 1a). The size of miR408 ranges from 20 to 22 bp, but most of the MIR408 precursors (n=142) generate 21 bp mature miR408 (Figure 1b and Table S1). Next, we have investigated the sequence conservation of the *MIR408* family at the level of mature and precursor levels in the plant kingdom. As expected, the mature miR408 showed high degree of conservation in across 97 plants species wherein the core miR408 is represented by 'UGCACUGCCUCUUCCCUGGC' (20 bp) except Han-miR408, Can-mir408, Sha-miR408 and Sly-miR408 where there in one SNP in core sequence (Figure S1b). The variations were observed at the 5′ and 3′ end respectively. The plant MIR408 family is represented by 14 mature sequence variants annotated across diverse plant groups (Figure 1c). The miR408-F3 (-UGCACUGCCUCUUCCCUGGCU--) is the most predominant, abundant and universal mature form arising from processing of 67 MIR408

Preprints (www.preprints.org) | NOT PEER-REVIEWED | Posted: 8 February 2022 doi:10.20944/preprints202202.0113.v1

precursor annotated in diverse plant species ranging from simpler bryophytes (*Physcomitrella patens*), spermatophytes (*Ginkgo biloba* and *Piceaabies*) to liliopsida (Araceae, Asparagaceae, Musaceae and Poaceae) to eudicots (Actinidiaceae, Asteraceae, Brassicaceae, Caricaceae, Convolvulaceae, Euphorbiaceae, Fabaceae, Malvacea, Nelumbonaceae, Oleaceae, Rosaceae, Rutaceae, Solanaceae, Amaranthaceae, Araliaceae, Apiaceae, Cleomaceae and Rhamnaceae) (Figure 1c). In addition, the other prominent miR408 mature form i.e., miR408-F-10 (AUGCACUGCCUCUUCCCUGGC--) was mostly present in Fabaceae (n=23) followed by other eudicots. Interestingly miR408-F-7 (CUGCACUGCCUCUUCCCUGGC--) was present only in poaceae (n=16). Other sequence variants were confined to only a few species (Figure 1c). As the different miR408 forms have variable 5′ base, the role of different AGOs in addition to AGO1 in miR408 loading in species-specific context is quite a possibility. The extensive conservation of mature miR408 across diverse plant groups suggests the indispensable function of miR408 in shaping key processes of plant development.

To assess the evolutionary conservation and diversification of *MIR408* family in plant kingdom, 156 MIR408 precursor sequences from 97 plant species were used as input for alignment followed by phylogenetic analysis using Maximum likelihood method and Tamura-Nel model in MEGA11 (Table S2). The MIR408 precursor alignment clearly demonstrated the peak conservation in and around the miRNA/miRNA* regions (Figure S2). The plant MIR408 family can be divided into 6 groups represented by lycophytes (G-I), Bryophytes (G-II), Gymnosperms (G-III), Malvales (G-IV), poales (G-V) and eudicots (G-VI) (Figure 1d). To our surprise the Tae-MIR408b was clustered together with Smo-MIR408s (lycophytes). The *Atr-MIR408* (*Amborellatrichopoda*) was distinct from other lycophytes and placed alone in the tree. While all the MIR408s from different species of malvaceae clustered together (G-IV) (Figure 1d). Most of the species of this family have four miR408 precursors. The MIR408 from all species belonging to poaceae were clustered together with nelumbonaceae and amaranthaceae in G-V. All other eudicots were represented in a giant cluster (G-VI) constituting several sub-clusters (VI-A to I) (Figure 1d). The sub-cluster VI-A constitute the MIR408 of Solanaceae family, represented by eight species. Another family-specific sub-cluster was seen for Brassicaceae (VI-F). Several species belonging to different dicot families were clubbed together in sub-cluster VI-I, wherein Fabaceae predominates the most (Figure 1d).

Preprints (www.preprints.org) | NOT PEER-REVIEWED | Posted: 8 February 2022 doi:10.20944/preprints202202.0113.v1

Comparative analysis of variations and haplotype evaluation in rice

The precursor and 1 Kb upstream cis-regulatory region (Ch01: 12300661 to 12301873) was analyzed for sequence variations (SNP and Indels) across 4726 rice accessions using the RiceVarMap2(http://ricevarmap.ncpgr.cn; Zhao et al. 2021[40]) database. As a result, a total of 22 sequence variants were detected, out of which 15 lies within the promoter while 7 lie in the putative precursor region downstream of mature (Figure 2a-b). Four variants (vg0112300662, vg0112300679, vg0112300683 and vg0112301149) that differ from reference represents the primary allele with frequency ranging from 0.647 to 0.678 (Figure 2a-b). In addition, other three variants (vg0112300734, vg0112300737, vg0112300779) were also very abundant in rice accessions. While eight variants represent low frequency and present in small subsets of rice accessions (vg0112300685, vg0112300704, vg0112301017, vg0112301021, vg0112301030, vg0112301098,vg0112301361 and vg0112301478) (Figure 2a-b). Next the overlap and intersection of the above variants were studied in relation to the presence of cis-regulatory motifs in the promoter region. Therefore, the promoter region was screened for different cis-regulatory motifs using New Place database (https://www.dna.affrc.go.jp/PLACE/?action=newplace;Higo et al. 1999[44]) and the resulted motifs were mapped on the promoter region using CLC genomics (Figure S3). Five variants i.e., vg-5,6,7,9 and 10 intersect with the several cis-regulatory motifs. Variant vg-5 overlaps in the SEF4 binding site (SEF4MOTIFGM7S) while vg-6 interferes with the Binding site of WRKY71 (WRKY71OS) and GTGA motif (GTGANTG10). Adjacently vg-7 overlaps with the binding sites of DOF proteins (DOFCOREZM). Interestingly vg-9 and 10 lie in the region with TATABOX5 and MARTBOX (Figure S3). The variants lie in the promoter were used to evaluate the haplotype using the Haplotype Network Analysis tool of RiceVarMap2. As a result, 8 haplotypes were calculated using following variants: vg0112300662, vg0112300679, vg0112300683, vg0112300685, vg0112300734, vg0112300779, vg0112301030 and vg0112301361 (Figure 2c-d). Haplotype I, IV and VIII were dominated by japonica accessions while hap-II, III, V,VI, VII were indica specific (Figure 2c-d).

Transcriptional and epigenetic regulation of miR408 in N22

In order to investigate the impact of different tissue types on regulation of miR408-target module under control as well as in drought conditions in tolerant rice cultivar, N22, the expression of miR408-3p was extracted from the small RNA sequencing data available for flag leaf, inflorescence and roots of N22 under control and drought conditions

Preprints (www.preprints.org) | NOT PEER-REVIEWED | Posted: 8 February 2022 doi:10.20944/preprints202202.0113.v1

(PRJNA294727). Under control conditions, miR408-3p was highly expressed in flag leaf (Figure 3a) as compared to roots and inflorescence. In flag leaf and roots of N22, miR408-3pwas upregulated while it showed slight downregulation in inflorescenceunder drought stress (Figure 3b). Then we examined the pre-MIR408 levels in roots and flag leaf of N22 under drought condition. Similar to the mature, the precursor was also upregulated in flag leaf and roots (Figure 3c). In summary miR408-3p exhibited differential expression in tissue as well in drought.

Further, to understand the role of DNA methylation in deriving the drought response of miR408-3p, the single base resolution of methylation levels was examined in all three tissues under control and drought conditions. For the above analysis the pre-*MIR408* along with 1kb cis-regulatory region was used and the differential methylation levels in different context (CpG, CHH and CHG) was extracted from in-house generated WGBS data available for flag leaf, inflorescence and root of N22 under drought stress. Clearly, no methylated cytosine (mCs) were observed in the promoter region while all the observed mCs lie in the precursor region (Figure 3d-e). Under control conditions higher fraction of mCs representing all three contexts were observed in inflorescence. In addition,mCs in CHG context was only observed in inflorescence and their fraction further increased under drought conditions (Figure 3d-e).While under drought conditions, the fraction of mCs in CpG and CHH context were increased in flag leaf as well as in roots. The enhanced fraction of mCs in CpG and CHH context in the precursor in flag leaf and root might be contributing towards the upregulation of miR408-3p under drought (Figure 3d-e).

Comparative expression analysis of miR408-3p/target module

To understand the diversity and conservation of genes targeted by miR408 in plants,the targets having evidence from degradome was obtained from PmiREN for *Oryza sativa*, *Arabidopsis*, *Brachypodium*, *Glycine max*, *Zea mays*, *Medicago*, *Physcomitrella patens*, tomato, potato, wheat, *Brassica napus*, *Selaginella moellendorffii* and *Vitis*. Phylogenetic analysis of all the above targets clearly showed the enrichment of the blue copper family as the dominant target class including the plastocyanin-like or the plantacyanins. In addition, laccases were also regulated by miR408 in Glycine max and tomato (Figure S4). A cluster of copper transporting ATPases as miR408 targets were also observed in *Zea mays*, tomato and *Arabidopsis* (Figure S4). Several genes encoding for Gycine rich proteins were also cleaved by miR408 in Brassica, rice, Arabidopsis and tomato (Figure S4). The above data suggest

 doi:10.20944/preprints202202.0113.v1

that the pool of miR408 targets is diverse with preference for genes encoding for blue copper family.

In rice, miR408-3p predominantly targets the plantacyanin family members,while several other targets belonging to diverse protein classes were predicted as well as identified through degradome analysis from diverse tissue types and cultivars. But in studies only few targets have been associated with miR408-mediated regulation (Pan et al. 2018[15]). Further, it is critical to understand how miR408-3p derives the differential regulation of its target transcripts in different tissue types and stress conditions. It's possible that miR408 may result in complete suppression of some targets while at the same time act as a rheostat for others to slightly dim their expression or even have no effect. The above relationship could also be impacted by basal expression of miR408-target node in different tissue typesvis-à-vis environmental conditions. Therefore, here in the present study efforts were directed to delineate the regulatory activity of miR408-3p on modulating its target transcripts by utilizing the comparative miRNome *vs.* transcriptome analysis in different tissues of N22 under drought stress. The miRNome and RNA-seq resources generated by our group were used to extract the miRNA-target expression in flag leaf, inflorescence and root under drought stress at the heading stage. The targets with evidence of cleavage by miR408-3p identified through degradome analysis were retrieved from the PmiREN database (category ≤2 and cleavage evidence from more than one degradome dataset). In total 119 genes were targeted by miR408-3p including its bona fide target gene family consisting of 11 plastocyanin-like domain containing proteins (Table S3). In addition, several other types of genes encoding different types of protein classes were also identified from the degradome data. Out of the 119 targets, 9 belong to the 0 category while 9 and 94 were among the category 1 and 2 respectively. Seven targets {LOC_Os03g49820.1 (score:2, expressed protein); LOC_Os01g02110.1 (score:2,helix-loop-helix DNA-binding domain containing protein), LOC_Os01g03530.1 (score: 1.5,multicopper oxidase domain containing protein), LOC_Os07g43540.1 (score:2, ORC6 - Putative origin recognition complex subunit 6), LOC_Os03g15340.1 (score: 0, plastocyanin-like domain containing protein), LOC_Os03g50140.1 (score: 1.5, plastocyanin-like domain containing protein), LOC_Os06g15600.1 (score: 1.5, plastocyanin-like domain containing protein)} with low alignment score were not identified in any of the degradome datasets, suggesting that they might exhibit expression restricted to some specific tissue or condition (Table S3). Nine target genes were supported by more than 10 degradome datasets including 5 plastocyanin-like domain containing protein (LOC_Os08g37670.1, LOC_Os09g29390.1,

Preprints (www.preprints.org) | NOT PEER-REVIEWED | Posted: 8 February 2022 doi:10.20944/preprints202202.0113.v1

LOC_Os06g11490.1, LOC_Os02g52180.1 and LOC_Os08g37660.1), drought-induced protein 1 (LOC_Os02g30320.1), periplasmic beta-glucosidase precursor (LOC_Os03g53800.3), expressed protein (LOC_Os02g49870.1) and ubiquitin family domain containing protein (LOC_Os01g68950.1). The GO enrichment analysis highlighted the putative role of miR408 targets in diverse biological processes and molecular function categories with significant enrichment of electron transfer activity and ETR chain, oxidoreductase activity etc. (Figure S5 a-c).

Further we analyzed how the transcriptional regulation of miR408-3p affected the repertoire of its target gene expression in different tissues types and stress, the RNA-seq datasets of flag leaf and root of our group's previous study (Gour et al. 2021[35]) was used. Considering the significant difference in the miR408-3p levels in flag leaf and roots, the transcript levels of targets were compared between flag leaf and roots to uncover the tissue specific target pool of miR408-3p (Figure 4a). Forty-nine (15 increased and 34 upregulated in roots) target genes exhibited opposite tissue-mediated expression pattern to that of miR408-3p (down regulated in roots)(Figure 4a). While 39 (6 decreased and 33 downregulated) followed similar expression pattern to miR408-3p suggesting that the difference in the miR408-3p expression modulate the levels of its target pool also (Figure 4a). Further, the comparative analysis was studied under drought conditions to see how the drought regulated transcriptional regulation of miR408-3p was reflected in drought response of its targettranscripts. In flag leaf out of 33 targets with significant fold change values, 14 targets followed significant downregulation and 5 genes exhibited reduced expression in response to drought in contrast to miR408-3p which was upregulated under drought in flag leaf (Figure 4c).However, 13 targets followed increased to upregulated expression similar to miR408-3p in flag leaf. In root, 38 targets (32 downregulated and 6 reduced) followed inverse expression trend, while 39 (33 upregulated and 6 increased) followed similar expression to miR408 (Figure 4b). Among the targets several genes followed tissue preferential expression in N22. Five genes followed flag leaf biased expression (FC ≥ 5in FL) viz. drought-induced protein 1 (LOC_Os02g30320), expressed protein (LOC_Os02g49870), catalase domain containing protein (LOC_Os03g03910), 2Fe-2S iron-sulfur cluster binding domain containing protein (LOC_Os07g30670) and thylakoid lumenal 29.8 kDa protein (LOC_Os12g08830) (Figure S5d). In contrast nine of miR408-targets exhibited inflorescence specific expression viz, Core histone H2A/H2B/H3/H4 domain containing protein (LOC_Os10g28230), Expressed protein (LOC_Os04g42200), Peroxidase precursor (LOC_Os03g13200), Plastocyanin-like domain containing protein (LOC_Os06g11490 and LOC_Os03g50140), Protein kinase

Preprints (www.preprints.org) | NOT PEER-REVIEWED | Posted: 8 February 2022 doi:10.20944/preprints202202.0113.v1

(LOC_Os07g07230), Retrotransposon protein (LOC_Os03g01930) and UP-9A (LOC_Os10g36580) (Figure S5d). Following 10 targets were highly expressed in roots as compared to flag leaf and inflorescence; AP2 domain containing protein (LOC_Os01g66270), Expressed protein (LOC_Os03g07590), Plastocyanin-like domain containing protein (LOC_Os08g37670, LOC_Os04g46130, LOC_Os03g50160, LOC_Os08g37660), 3-ketoacyl-CoA synthase (LOC_Os02g11070), AP2 domain containing protein (LOC_Os06g07030), Glycine-rich cell wall structural protein 2 precursor (LOC_Os10g31660) and Helix-loop-helix DNA-binding domain containing protein (LOC_Os01g02110) (Figure 3d). Interestingly, several of the root specific miR408-3p targets also exhibited inverse drought regulation to that of miR408-3p. Therefore, to validate the expression profiles of MIR408/target modules in root, 5 genes with root preferential drought mediated downregulation were selected and analyzed though qRT-PCR (Figure 4d). The results confirmed the downregulation of all five genes in root while the *MIR408* exhibited upregulation upon drought in roots (Figure 4d). From the above observations, it was clear that miR408 regulates unique set of targets in different tissues and with variable magnitude.

Expression analysis of miR408-3p targets in MIR408-OE plants

To further study the impact of miR408-3p overexpression on its target transcripts the RNA-seq data of seedlings of MIR408 overexpression and wild type rice were downloaded from NCBI (BioProject PRJNA412295; Zhang et al. 2017[16]) followed by RNA-seq analysis using CLC genomics. The differential expression of MIR408 and its targets were extracted and the relative fold expression in MIR408-OE w.r.t. to wild type was calculated. In the MIR408-OE line the MIR408 was 8 times upregulated confirming the optimum level of overexpression in lines. Out of 119 target genes,11 (LOC_Os04g46130, LOC_Os02g52180, LOC_Os08g37670, LOC_Os06g11490, LOC_Os02g06530, LOC_Os03g50160, LOC_Os03g15340, LOC_Os03g09940, LOC_Os03g01930, LOC_Os10g36580 and LOC_Os03g07590) exhibited significant downregulation (FC ≤ 0.5) in MIR408-OE (Figure 4e). Twenty-one targets were reduced to a FC range of 0.80≤ to ≥0.50 in MIR408-OE. While a large number of targets i.e., 61 showed non-differential expression pattern in MIR408-OE. Moreover 17 targets observed to be slightly upregulated upon MIR408 overexpression (Figure 4e and S6).

To summarize the miR408-target regulatory relationship across different tissues, overexpression lines and drought, comparative intersection of targets following the inverse

Preprints (www.preprints.org) | NOT PEER-REVIEWED | Posted: 8 February 2022 doi:10.20944/preprints202202.0113.v1

expression to miR408 was studied. The data suggest the coherent co-expression of miR408-target module in all tissues but both miR408 and some targets do exhibit tissue preference (Figure S6). Further the dynamic selection and miR408-mediated regulation or the degree of expression anticorrelation of target nodes were modulated by the tissue types and stress conditions. Out of 119 targets, 83 showed antagonistic expression to miR408-3p in either of studied domains (Figure 4f). One target gene encoding for pirin (LOC_Os08g27720) exhibited antagonistic expression with miR408-3p in all four contexts. Another set of 11 genes followed anticorrelation in three conditions including few roots specific targets (Figure 4f).Twenty-five targets are significantly modulated by the tissue mediated (FL to RT) as well drought mediated dynamic shift in the expression of miR408-3p in roots. The above observation highlights the critical role miR408-3p in shaping the root's target pool at tissue as well as at stress tolerance level. Twenty-seven showed anticorrelation in any two conditions (Figure 4f). While large number of targets were only observed to be regulated in opposite manner in one condition e.g., 10 in FL (drought), 11 in MIR408-OE, 9 in RT (drought) and 14 in tissue biased manner (RT/FL) (Figure S6). The above data demonstrated the impact of tissue and stress on the mode of miR408-directed regulation of target transcript suggesting that at a particular set of conditions miR408 derives significant clearance of some targets while may act as buffering agent for others to eliminate the noise.

High levels of miR408 enhances the vegetative vigour and water stress tolerance of the drought sensitive rice

Our present and previous data (Balyan et al. 2017[28]) clearly demonstrated the important role of miR408-target module in drought stress response of rice cultivars. Considering the drought tolerant cultivar-specific expression of miR408 and lack of evidence of miR408-OE mediated drought tolerance, over-expressed MIR408 lines were generated in the drought-sensitive cultivar, PB1 (Figure S7). Four transgenic lines were obtained and subjected to in-depth phenotypic analysis (Figure S7). The Over-expression lines exhibited variable magnitude of miR408 upregulation (Figure S7b) and highest overexpression was observed for MIR408-OE-16 (~ 16 fold; Figure S7b). All the four MIR408-OE lines exhibited significant increments in shoot length, root length and seedling weight suggesting miR408 as a positive regulator of rice growth and vigor (Figure S7). In comparison to other MIR408-OE lines, line 16 showed highest growth enhancement and miR408-3p expression, therefore MIR408-OE was selected for further investigation at T2 generation. Comprehensive morphometric analysis of 40 day old WT and MIR408-OE-16 plants clearly showed the role

Preprints (www.preprints.org) | NOT PEER-REVIEWED | Posted: 8 February 2022 doi:10.20944/preprints202202.0113.v1

of miR408-3p in enhancing vegetative growth and development of rice plants (Figure 5). Plants show vigorous growth and reach the 4-leaf-stage whereas control plants reach only 3-leaf-stage (Figure 5a-b).There is significant increase in shoot length, seedling fresh weight, root length as well as the root density (Figure 5c-f). Besides increase in the leaf blade length there is a significant increase in the leaf blade width as well (Figure 5g-i). The chlorophyll content (chlorophyll 'a'&'b') increased by as much as 20-25 % (Figure 5j). While the maximum photosynthetic efficiency (Fv/Fm) is similar there was a significant increase in the effective photosynthetic efficiency Y(II) and electron transfer rate (ETR) in the over-expression lines even under normal growth conditions (Figure 5k and l).

At molecular level, the expression of seven degradome identified targets were analysed in MIR408-OE-16 plants. As expected five (LOC_Os03g15340, LOC_Os08g37670, LOC_Os02g43660, LOC_Os06g15600, LOC_Os03g50160, LOC_Os06g11490, LOC_Os09g29390) targets were downregulated while LOC_Os08g37670remained non-differential (Figure 5m). Surprisingly LOC_Os03g50160 was upregulated in MIR408-OE plants (Figure 5m).

As miR408-3p followed cultivar-biased drought regulation and upregulated in tolerant cultivars while downregulated in sensitive ones (Balyan et al. 2017[28]). The WT and MIR408-OE plants were screened for dehydration stress (20% PEG) tolerance at seedling stage (Figure 6). After 1 h of stress (20% PEG solution) clear leaf rolling with needle like appearance was visible in wild type plants (Figure 6). In contrast, the leaves of MIR408-OE, had just started to roll from tips and no needle-like leaf was seen (Figure 6a-d). Even after 7 h, MIR408-OE plants were in better condition with some expanded leaves (Figure 6e). Further, transgenic plants performed better than wild type plants during recovery (Figure 6f). The transgenic lines also showed slightly higher relative water content (Figure 5g) and maintained stable Fv/Fm values (Figure 6h) after 7 h of PEG treatment. Interestingly, although there is an overall decrease in the Y(II) and ETR in both WT and the transgenic plants, the Y(II) and ETR of transgenic plants were maintained at higher levels than the wild type plants (Figure 6i-j). Although the seedling weight decreased in stress conditions in both WT and MIR408-OE, the MIR408-OE maintained higher mass as compared to WT in stress conditions (Figure 6k). The above data suggested the role of miR408-3p as a positive regulator of growth, development and water stress tolerance in rice.

Discussion

Preprints (www.preprints.org) | NOT PEER-REVIEWED | Posted: 8 February 2022 doi:10.20944/preprints202202.0113.v1

Several miRNA families in plants are conserved across the diverse lineages while the majority are confined to some specific group or species (Cuperus et al. 2011[10]). MIR156, MIR159, MIR160, MIR166, MIR171, MIR390, MIR408 and MIR395 are present in all plant lineages while several others displayed restricted taxonomic conservation e.g. MIR528 (monocots), MIR472 (Rosids) and MIR857 (Eurosids) (Cuperus et al. 2011[10]). MIR408 was one such conserved miRNA family that was reported to have a key role in mechanisms regulating growth, development, stress response and nutritional requirements (Ma et al. 2015[45]; Hang et al. 2021[24]; Song et al. 2018[21]; Zhang et al. 2017[16]; Pan et al. 2018[15]). The present study investigated the MIR408 taxonomic conservation across plant kingdom followed by in-depth characterization of expression dynamics of miR408-target modules in drought stress in rice. Further overexpression of MIR408 enhanced the vigor, photosynthesis and dehydration stress tolerance of drought sensitive rice suggesting the role of miR408 as positive key regulator of both rice growth and dehydration response.

MIR408 is highly conserved across plants

MIR408 was shown to be taxonomically conserved across plants (Pan et al. 2018 [15]and Hang et al. 2020[24]) but the support was from a limited number of species. Recently the extensive annotation of MIRNA genes in plants was done by several groups and catalogued in different databases, providing an excellent opportunity to study the evolutionary conservation and diversification of miRNAs in plants. We utilized the 156 *MIR408* precursors from 97 plant species representing different taxonomic groups of plants from bryophytes to eudicots, for detailed comparative sequence analysis at mature and precursor level. MIR408 was absent from chlorophytes and originated in bryophytes as suggested by its presence in *Marchantia polymorpha* and *Physcomitrella patens* (sRNAnno and PmiREN). Unlike multigene conserved families like MIR156 and MIR172, MIR408 is represented by only single precursor in majority of species (63) while in several species expansion did happen as evidenced from multiple MIR408 members e.g. wheat where six MIR408 members has been annotated. The plant miRNAs family members derived from the same family are mostly similar at mature as well as at precursor levels suggesting their recent and still progressing expansion (Li and Mao 2007[46]). Here also the different precursors of MIR408 and mature sequence share high homology within a species suggesting their origin due to tandem duplications. Further the ~92 % of MIR408 precursors processed into 21 bp mature miR408 while 20 and 22 bp mature were also found in some species. The mature sequence is fairly preserved and the divergence was only restricted to 5 and 3' ends. Further the plant

Preprints (www.preprints.org) | NOT PEER-REVIEWED | Posted: 8 February 2022 doi:10.20944/preprints202202.0113.v1

MIR408 can be divided into 14 mature sequence variants, out of which three forms i.e. MIR408-F3, 7 and 10 dominate over other forms. miR408-F-7 (CUGCACUGCCUCUUCCCUGGC--) was observed to be confined to only species belonging to poaceae while miR408-F-10 (AUGCACUGCCUCUUCCCUGGC--) was mostly seen in Fabaceae. While the most abundant miR408-F3 (-UGCACUGCCUCUUCCCUGGCU--) showed ubiquitous distribution across different plant groups. As the above three forms differ in 5' base it's interesting to investigate the involvement of different AGO proteins in miR408 loading in species dependent manner. miR408 was reported to be associated with both AGO1 and AGO2 in Arabidopsis (Maunoury and Vaucheret 2011[47]). The origin and activity of isomiRs processed from several miRNAs including miR408 was reported in rice (Balyan et al. 2020[48]). At the level of precursor also the regions around the miR408 and miR408* exhibited extensive conservation. The course of evolution through phylogenetic analysis suggested the origin of MIR408 in bryophytes followed by gymnosperms. The MIR408 from basal eudicot *Nelumbo Nucifera* was shared homology with the poaceae specific clade. The malvaceae clade seems to be more ancient than other eudicots. The giant dicot clade was further divided into sub-clades.

miR408-target modules exhibited differential tissue/ drought-mediated regulation in rice

In our previous study we have reported the drought tolerant cultivar-specific upregulation of miR408-3p in flag leaf (Balyan et al. 2017[28]; Mutum et al. 2013[29]). Here the comparative expression profile of miR408-3p in flag leaf, roots and inflorescence of N22 showed that it was expressed in higher amounts in flag leaf and low levels were maintained in roots. Further miR408-3p followed upregulated expression in roots and flag leaf under drought due to the transcriptional upregulation of its precursor in both the tissues. Further OsSPL9 was known to regulate the transcriptional activation of miR408-3p under copper starvation conditions (Balyan et al. 2017[28]). Other than that, the transcriptional regulation of *MIR408* is yet to be uncovered in rice. Dynamic DNA methylation is critical in shaping transcriptome of rice under natural as well as under specific environmental conditions including drought (Rajkumar et al. 2020[49]; Wang et al. 2016[50]). But still only a handful of reports demonstrated the role and impact of DNA methylation on the transcriptional regulation of MIR genes in plants (Ci et al. 2015[51]; Rambani et al. 2020[52]). Here the comparative single base methylation levels, mCs in the promoter and MIR408 gene body in

 doi:10.20944/preprints202202.0113.v1

flag leaf, root and inflorescence under control and stress conditions suggest role of epigenetic regulation of MIR408 loci in N22. The dynamic methylation sites were only identified in the MIR408 gene body and not in the promoter. mCs in CpG and CHH context are prevalent in all three tissues but CHG context was specific to inflorescence only. Also, the significant increase in the fraction of mCs in CpG and CHH context under drought in both roots and flag leaf followed positive correlation with the miR408-3p expression. The positive correlation between the expression and the methylation levels in the gene body were also observed in previous reports also (Liang et al. 2019[53]; Wang et al. 2016[50]).

Importantly, the above observed tissue-mediated drought responsive differential expression of miR408-3p mediates the post-transcriptional regulation of their target pool differentially depending on stress, tissue and stage of development. The differential pools of targets are regulated by miR408-3p at the level of tissue (RT vs. flag leaf), drought stress (in roots and flag leaf) and *MIR408* overexpression (seedling stage). Several miR408 targets followed tissue preferential expression including some of the top category targets which exhibited root specific expression in N22. The tissue-restricted expression could be one of the reasons for the non-identification of targets in a degradome with very low alignment scores. This suggests that the cellular context plays an important role in regulating the miR408-3p/target pool in N22. Recent report showed that the patterns and levels of miRNAs in maize are largely determined at the level of transcription and finely tuned post-transcriptionally in a tissue dependent manner (Ma et al. 2021[45]). Based on the condition/tissue specific target expression versatility 83 targets have been identified with inverse expression to miR408 in at least one condition. Further, 12 targets are regulated inversely in most conditions suggesting the critical role of miR408-3p in post-trancriptional regulation of these targets. The above candidates include novel miR408 targets that were unreported in previous reports. A total of 50 miR408-3p/target nodes were responsive to drought, while 49 showed modulation even change in cellular context.

MIR408 is a positive regulator of drought and vegetative growth in rice

Further insight into the functionality of MIR408 was gained by over-expressing miR408 in the drought-sensitive rice cultivar (PB1) to explore the impact of elevated levels of miR408 on rice growth and stress tolerance. Indeed, the transgenic plants were more vigorous than wild type plants with enhanced root length, number of lateral roots, shoot length, leaf width and seedling weight along with increased chlorophyll. Interestingly, there was no noticeable effect on the Fv/Fm in the transgenic plants but there is significant increase in the ETR and Y

 doi:10.20944/preprints202202.0113.v1

(II) values as compared to the wild type PB1 plants. In *Arabidopsis,* MIR408 over-expressing plants showed higher chlorophyll and plastocyanin levels due to increased copper delivery (Zhang et al., 2017[16]). Plastocyanin levels are known to affect plant vegetative growth and photosynthesis (Weigel et al., 2003[54]; Pesaresi et al., 2009[55]). In rice the miR408-UCL8 (LOC_Os03g50140) was involved in enhancing grain yield, panicle branching, grain number and photosynthesis (Zhang et al. 2017[16]). UCL8 showed high enrichment in pistil, young panicles, seeds and inflorescence meristem (Zhang et al. 2018[14]). In the present study also UCL8 was inflorescence enriched but it did not follow drought mediated inverse expression in N22. The enhanced growth parameters were in concordance with the results obtained for MIR408 overexpression in rice, Arabidopsis, and tobacco (Song et al. 2018[21]; Pan et al. 2018[15]). As miR408 was downregulated in drought sensitive cultivar reported by our previous report, we want to see whether the over-expression lines performed better than the WT when challenged with dehydration stress by PEG. Enhanced ETR is associated with higher photosynthesis, plant growth and tolerance to oxidative stress (Chida et al., 2007[56]). Drought tolerant wheat genotypes maintain better ETR levels than the sensitive one under drought (Subrahmanyam et al., 2006[57]). Also miR408 overexpression in displayed improved thermotolerance in ryegrass, drought tolerance in ryegrass, drought and salinity tolerance in cowpea and are important in wounding response in sweet potato. But the direct role of miR408 in improving drought tolerance in high yielding drought sensitive rice backgrounds is still lacking. Thus, tolerance of miR408-overexpression transgenic plants could be attributed to the enhanced growth and higher basal levels of ETR and Y(II) even under stress. Enhanced ETR is associated with higher photosynthesis, plant growth, tolerance to oxidative stress (Chida et al., 2007[56]; Takahara et al., 2010[58]) and drought tolerance (Wang et al., 2014[59]), as was observed in our study also.

Author Contributions

SR conceived the research and supervised the experiments; SB executed all the experiments and analysed the data;; SK and RJ analysed the methylation status of MIR408 region; PB performed the phylogenetic analysis of targets; RC complemented the expression analysis; SR and SB wrote the manuscript.

Conflicts of Interest

There is no conflict of interest among the authors

References

1. Nadarajah, K.; Kumar, I.S. Drought Response in Rice: The MiRNA Story. *Int. J. Mol. Sci.***2019**, *20*, 3766, doi:10.3390/ijms20153766.
2. Kansal, S.; Devi, R.M.; Balyan, S.C.; Arora, M.K.; Singh, A.K.; Mathur, S.; Raghuvanshi, S. Unique MiRNome during Anthesis in Drought-Tolerant Indica Rice Var. Nagina 22. *Planta***2015**, *241*, doi:10.1007/s00425-015-2279-3.
3. Singroha, G.; Sharma, P.; Sunkur, R. Current Status of MicroRNA-Mediated Regulation of Drought Stress Responses in Cereals. *Physiol. Plant.***2021**, *172*, doi:10.1111/ppl.13451.
4. Ni, Z.; Hu, Z.; Jiang, Q.; Zhang, H. Overexpression of Gma-MIR394a Confers Tolerance to Drought in Transgenic Arabidopsis Thaliana. *Biochem. Biophys. Res. Commun.***2012**, *427*, doi:10.1016/j.bbrc.2012.09.055.
5. Jiao, Z.; Lian, C.; Han, S.; Huang, M.; Shen, C.; Li, Q.; Niu, M.X.; Yu, X.; Yin, W.; Xia, X. PtmiR169o Plays a Positive Role in Regulating Drought Tolerance and Growth by Targeting the PtNF-YA6 Gene in Poplar. *Environ. Exp. Bot.***2021**, *189*, doi:10.1016/j.envexpbot.2021.104549.
6. Li, J.; Duan, Y.; Sun, N.; Wang, L.; Feng, S.; Fang, Y.; Wang, Y. The MiR169n-NF-YA8 Regulation Module Involved in Drought Resistance in Brassica Napus L. *Plant Sci.***2021**, *313*, doi:10.1016/j.plantsci.2021.111062.
7. Ferdous, J.; Whitford, R.; Nguyen, M.; Brien, C.; Langridge, P.; Tricker, P.J. Drought-Inducible Expression of Hv-MiR827 Enhances Drought Tolerance in Transgenic Barley. *Funct. Integr. Genomics***2017**, *17*, doi:10.1007/s10142-016-0526-8.
8. Zhang, X.; Zou, Z.; Gong, P.; Zhang, J.; Ziaf, K.; Li, H.; Xiao, F.; Ye, Z. Over-Expression of MicroRNA169 Confers Enhanced Drought Tolerance to Tomato. *Biotechnol. Lett.***2011**, *33*, 403–409, doi:10.1007/s10529-010-0436-0.
9. Zhang, J.; Zhang, H.; Srivastava, A.K.; Pan, Y.; Bai, J.; Fang, J.; Shi, H.; Zhu, J.K. Knockdown of Rice MicroRNA166 Confers Drought Resistance by Causing Leaf Rolling and Altering Stem Xylem Development. *Plant Physiol.***2018**, *176*, doi:10.1104/pp.17.01432.
10. Cuperus, J.T.; Fahlgren, N.; Carrington, J.C. Evolution and Functional Diversification of MIRNA Genes. *PLANT CELL ONLINE***2011**, doi:10.1105/tpc.110.082784.
11. Axtell, M.J.; Snyder, J.A.; Bartel, D.P. Common Functions for Diverse Small RNAs of Land Plants. *Plant Cell***2007**, *19*, doi:10.1105/tpc.107.051706.

12. Samad, A.F.A.; Sajad, M.; Nazaruddin, N.; Fauzi, I.A.; Murad, A.M.A.; Zainal, Z.; Ismail, I. MicroRNA and Transcription Factor: Key Players in Plant Regulatory Network. *Front. Plant Sci.***2017**, *8*, doi:10.3389/fpls.2017.00565.
13. Kozomara, A.; Griffiths-Jones, S. MiRBase: Annotating High Confidence MicroRNAs Using Deep Sequencing Data. *Nucleic Acids Res.***2014**, *42*, doi:10.1093/nar/gkt1181.
14. Zhang, F.; Zhang, Y.C.; Zhang, J.P.; Yu, Y.; Zhou, Y.F.; Feng, Y.Z.; Yang, Y.W.; Lei, M.Q.; He, H.; Lian, J.P.; et al. Rice UCL8, a Plantacyanin Gene Targeted by MiR408, Regulates Fertility by Controlling Pollen Tube Germination and Growth. *Rice***2018**, *11*, doi:10.1186/s12284-018-0253-y.
15. Pan, J.; Huang, D.; Guo, Z.; Kuang, Z.; Zhang, H.; Xie, X.; Ma, Z.; Gao, S.; Lerdau, M.T.; Chu, C.; et al. Overexpression of MicroRNA408 Enhances Photosynthesis, Growth, and Seed Yield in Diverse Plants. *J. Integr. Plant Biol.***2018**, *60*, doi:10.1111/jipb.12634.
16. Zhang, J.P.; Yu, Y.; Feng, Y.Z.; Zhou, Y.F.; Zhang, F.; Yang, Y.W.; Lei, M.Q.; Zhang, Y.C.; Chen, Y.Q. MiR408 Regulates Grain Yield and Photosynthesis via a Phytocyanin Protein. *Plant Physiol.***2017**, *175*, doi:10.1104/pp.17.01169.
17. Zhang, H.; Li, L. SQUAMOSA Promoter Binding Protein-Like7 Regulated MicroRNA408 Is Required for Vegetative Development in Arabidopsis. *Plant J.***2013**, *74*, doi:10.1111/tpj.12107.
18. Yamasaki, H.; Hayashi, M.; Fukazawa, M.; Kobayashi, Y.; Shikanai, T. *SQUAMOSA* Promoter Binding Protein–Like7 Is a Central Regulator for Copper Homeostasis in *Arabidopsis*. *Plant Cell***2009**, *21*, 347–361, doi:10.1105/tpc.108.060137.
19. Jiang, A.; Guo, Z.; Pan, J.; Yang, Y.; Zhuang, Y.; Zuo, D.; Hao, C.; Gao, Z.; Xin, P.; Chu, J.; et al. The PIF1-MiR408-PLANTACYANIN Repression Cascade Regulates Light-Dependent Seed Germination. *Plant Cell***2021**, *33*, doi:10.1093/plcell/koab060.
20. Zhang, H.; Zhao, X.; Li, J.; Cai, H.; Deng, X.W.; Li, L. Microrna408 Is Critical for the HY5-SPl7 Gene Network That Mediates the Coordinated Response to Light and Copper. *Plant Cell***2014**, *26*, doi:10.1105/tpc.114.127340.
21. Song, Z.; Zhang, L.; Wang, Y.; Li, H.; Li, S.; Zhao, H.; Zhang, H. Constitutive Expression of Mir408 Improves Biomass and Seed Yield in Arabidopsis. *Front. Plant Sci.***2018**, *8*, doi:10.3389/fpls.2017.02114.
22. Zhao, X.Y.; Hong, P.; Wu, J.Y.; Chen, X.B.; Ye, X.G.; Pan, Y.Y.; Wang, J.; Zhang, X.S. The Tae-MiR408-Mediated Control of TaTOC1 Genes Transcription Is Required

for the Regulation of Heading Time in Wheat. *Plant Physiol.***2016**, *170*, doi:10.1104/pp.15.01216.

23. Mishra, S.; Sahu, G.; Shaw, B.P. Integrative Small RNA and Transcriptome Analysis Provides Insight into Key Role of MiR408 towards Drought Tolerance Response in Cowpea. *Plant Cell Rep.***2021**, doi:10.1007/s00299-021-02783-5.
24. Hang, N.; Shi, T.; Liu, Y.; Ye, W.; Taier, G.; Sun, Y.; Wang, K.; Zhang, W. Overexpression of Os-MicroRNA408 Enhances Drought Tolerance in Perennial Ryegrass. *Physiol. Plant.***2021**, *172*, doi:10.1111/ppl.13276.
25. Hajyzadeh, M.; Turktas, M.; Khawar, K.M.; Unver, T. MiR408 Overexpression Causes Increased Drought Tolerance in Chickpea. *Gene***2015**, *555*, doi:10.1016/j.gene.2014.11.002.
26. Taier, G.; Hang, N.; Shi, T.; Liu, Y.; Ye, W.; Zhang, W.; Wang, K. Ectopic Expression of Os-Mir408 Improves Thermo-Tolerance of Perennial Ryegrass. *Agronomy***2021**, *11*, doi:10.3390/agronomy11101930.
27. Guo, Y.; Wang, S.; Yu, K.; Xu, H.; Song, C.; Zhao, Y.; Wen, J.; Fu, C.; Li, Y.; Zhang, X.; et al. MicroRNA408 Enhances Growth and Saccharification Efficiency Through Altering the Balance between Vascular Development and Lignification in Hybrid Poplar. *SSRN Electron. J.***2021**, doi:10.2139/ssrn.3850364.
28. Balyan, S.; Kumar, M.; Mutum, R.D.; Raghuvanshi, U.; Agarwal, P.; Mathur, S.; Raghuvanshi, S. Identification of MiRNA-Mediated Drought Responsive Multi-Tiered Regulatory Network in Drought Tolerant Rice, Nagina. *Sci. Rep.***2017**, *7*, doi:10.1038/s41598-017-15450-1.
29. Mutum, R.D.; Balyan, S.C.; Kansal, S.; Agarwal, P.; Kumar, S.; Kumar, M.; Raghuvanshi, S. Evolution of Variety-Specific Regulatory Schema for Expression of Osa-MiR408 in Indica Rice Varieties under Drought Stress. *FEBS J.***2013**, *280*, doi:10.1111/febs.12186.
30. Tamura, K.; Stecher, G.; Kumar, S. MEGA11: Molecular Evolutionary Genetics Analysis Version 11. *Mol. Biol. Evol.***2021**, *38*, doi:10.1093/molbev/msab120.
31. Guo, Z.; Kuang, Z.; Zhao, Y.; Deng, Y.; He, H.; Wan, M.; Tao, Y.; Wang, D.; Wei, J.; Li, L.; et al. PmiREN2.0: From Data Annotation to Functional Exploration of Plant MicroRNAs. *Nucleic Acids Res.***2021**, doi:10.1093/nar/gkab811.
32. Guindon, S.; Dufayard, J.-F.; Lefort, V.; Anisimova, M.; Hordijk, W.; Gascuel, O. New Algorithms and Methods to Estimate Maximum-Likelihood Phylogenies: Assessing the Performance of PhyML 3.0. *Syst. Biol.***2010**, *59*, 307–321, doi:10.1093/sysbio/syq010.

33. Ro, S.; Park, C.; Jin, J.; Sanders, K.M.; Yan, W. A PCR-Based Method for Detection and Quantification of Small RNAs. *Biochem. Biophys. Res. Commun.***2006**, *351*, 756–763, doi:10.1016/j.bbrc.2006.10.105.
34. Ge, S.X.; Jung, D.; Jung, D.; Yao, R. ShinyGO: A Graphical Gene-Set Enrichment Tool for Animals and Plants. *Bioinformatics***2020**, *36*, doi:10.1093/bioinformatics/btz931.
35. Gour, P.; Kansal, S.; Agarwal, P.; Mishra, B.S.; Sharma, D.; Mathur, S.; Raghuvanshi, S. Variety-specific Transcript Accumulation during Reproductive Stage in Drought-stressed Rice. *Physiol. Plant.***2021**, doi:10.1111/ppl.13585.
36. Lawrence, M.; Huber, W.; Pagès, H.; Aboyoun, P.; Carlson, M.; Gentleman, R.; Morgan, M.T.; Carey, V.J. Software for Computing and Annotating Genomic Ranges. *PLoSComput. Biol.***2013**, *9*, e1003118, doi:10.1371/journal.pcbi.1003118.
37. Yu, G.; Wang, L.-G.; He, Q.-Y. ChIPseeker: An R/Bioconductor Package for ChIP Peak Annotation, Comparison and Visualization. *Bioinformatics***2015**, *31*, 2382–2383, doi:10.1093/bioinformatics/btv145.
38. Toki, S.; Hara, N.; Ono, K.; Onodera, H.; Tagiri, A.; Oka, S.; Tanaka, H. Early Infection of Scutellum Tissue with *Agrobacterium* Allows High-Speed Transformation of Rice. *Plant J.***2006**, *47*, 969–976, doi:10.1111/j.1365-313X.2006.02836.x.
39. Dansana, P.K.; Kothari, K.S.; Vij, S.; Tyagi, A.K. OsiSAP1 Overexpression Improves Water-Deficit Stress Tolerance in Transgenic Rice by Affecting Expression of Endogenous Stress-Related Genes. *Plant Cell Rep.***2014**, *33*, 1425–1440, doi:10.1007/s00299-014-1626-3.
40. Zhao, H.; Li, J.; Yang, L.; Qin, G.; Xia, C.; Xu, X.; Su, Y.; Liu, Y.; Ming, L.; Chen, L.L.; et al. An Inferred Functional Impact Map of Genetic Variants in Rice. *Mol. Plant***2021**, *14*, doi:10.1016/j.molp.2021.06.025.
41. Chen, C.; Li, J.; Feng, J.; Liu, B.; Feng, L.; Yu, X.; Li, G.; Zhai, J.; Meyers, B.C.; Xia, R. SRNAanno—a Database Repository of Uniformly Annotated Small RNAs in Plants. *Hortic. Res.***2021**, *8*, doi:10.1038/s41438-021-00480-8.
42. Kozomara, A.; Birgaoanu, M.; Griffiths-Jones, S. MiRBase: From MicroRNA Sequences to Function. *Nucleic Acids Res.***2019**, *47*, doi:10.1093/nar/gky1141.
43. Feng, H.; Zhang, Q.; Wang, Q.; Wang, X.; Liu, J.; Li, M.; Huang, L.; Kang, Z. Target of Tae-MiR408, a Chemocyanin-like Protein Gene (TaCLP1), Plays Positive Roles in Wheat Response to High-Salinity, Heavy Cupric Stress and Stripe Rust. *Plant Mol. Biol.***2013**, *83*, doi:10.1007/s11103-013-0101-9.

44. Higo, K.; Ugawa, Y.; Iwamoto, M.; Korenaga, T. Plant Cis-Acting Regulatory DNA Elements (PLACE) Database: 1999. *Nucleic Acids Res.***1999**, *27*, 297–300, doi:10.1093/nar/27.1.297.
45. Ma, C.; Burd, S.; Lers, A. MiR408 Is Involved in Abiotic Stress Responses in Arabidopsis. *Plant J.***2015**, *84*, doi:10.1111/tpj.12999.
46. Li, A.; Mao, L. Evolution of Plant MicroRNA Gene Families. *Cell Res.***2007**, *17*, doi:10.1038/sj.cr.7310113.
47. Maunoury, N.; Vaucheret, H. AGO1 and AGO2 Act Redundantly in MiR408-Mediated Plantacyanin Regulation. *PLoS ONE***2011**, *6*, doi:10.1371/journal.pone.0028729.
48. Balyan, S.; Joseph, S.V.; Jain, R.; Mutum, R.D.; Raghuvanshi, S. Investigation into the MiRNA/5' IsomiRNAs Function and Drought-Mediated MiRNA Processing in Rice. *Funct. Integr. Genomics***2020**, *20*, doi:10.1007/s10142-020-00731-2.
49. Rajkumar, M.S.; Shankar, R.; Garg, R.; Jain, M. Bisulphite Sequencing Reveals Dynamic DNA Methylation under Desiccation and Salinity Stresses in Rice Cultivars. *Genomics***2020**, *112*, 3537–3548, doi:10.1016/j.ygeno.2020.04.005.
50. Wang, W.; Qin, Q.; Sun, F.; Wang, Y.; Xu, D.; Li, Z.; Fu, B. Genome-Wide Differences in DNA Methylation Changes in Two Contrasting Rice Genotypes in Response to Drought Conditions. *Front. Plant Sci.***2016**, *7*, doi:10.3389/fpls.2016.01675.
51. Ci, D.; Song, Y.; Tian, M.; Zhang, D. Methylation of MiRNA Genes in the Response to Temperature Stress in Populus Simonii. *Front. Plant Sci.***2015**, *6*, doi:10.3389/fpls.2015.00921.
52. Rambani, A.; Hu, Y.; Piya, S.; Long, M.; Rice, J.H.; Pantalone, V.; Hewezi, T. Identification of Differentially Methylated MiRNA Genes During Compatible and Incompatible Interactions Between Soybean and Soybean Cyst Nematode. *Mol. Plant-Microbe Interactions*®**2020**, *33*, 1340–1352, doi:10.1094/MPMI-07-20-0196-R.
53. Liang, L.; Chang, Y.; Lu, J.; Wu, X.; Liu, Q.; Zhang, W.; Su, X.; Zhang, B. Global Methylomic and Transcriptomic Analyses Reveal the Broad Participation of DNA Methylation in Daily Gene Expression Regulation of Populus Trichocarpa. *Front. Plant Sci.***2019**, *10*, 243, doi:10.3389/fpls.2019.00243.
54. Weigel, M.; Varotto, C.; Pesaresi, P.; Finazzi, G.; Rappaport, F.; Salamini, F.; Leister, D. Plastocyanin Is Indispensable for Photosynthetic Electron Flow in Arabidopsis Thaliana. *J. Biol. Chem.***2003**, *278*, doi:10.1074/jbc.M302876200.
55. Pesaresi, P.; Scharfenberg, M.; Weigel, M.; Granlund, I.; Schröder, W.P.; Finazzi, G.; Rappaport, F.; Masiero, S.; Furini, A.; Jahns, P.; et al. Mutants, Overexpressors, and

Interactors of Arabidopsis Plastocyanin Isoforms: Revised Roles of Plastocyanin in Photosynthetic Electron Flow and Thylakoid Redox State. *Mol. Plant***2009**, *2*, doi:10.1093/mp/ssn041.

56. Chida, H.; Nakazawa, A.; Akazaki, H.; Hirano, T.; Suruga, K.; Ogawa, M.; Satoh, T.; Kadokura, K.; Yamada, S.; Hakamata, W.; et al. Expression of the Algal Cytochrome C6 Gene in Arabidopsis Enhances Photosynthesis and Growth. *Plant Cell Physiol.***2007**, *48*, 948–957, doi:10.1093/pcp/pcm064.
57. Subrahmanyam, D.; Subash, N.; Haris, A.; Sikka, A.K. Influence of Water Stress on Leaf Photosynthetic Characteristics in Wheat Cultivars Differing in Their Susceptibility to Drought. *Photosynthetica***2006**, *44*, doi:10.1007/s11099-005-0167-y.
58. Takahara, K.; Kasajima, I.; Takahashi, H.; Hashida, S.; Itami, T.; Onodera, H.; Toki, S.; Yanagisawa, S.; Kawai-Yamada, M.; Uchimiya, H. Metabolome and Photochemical Analysis of Rice Plants Overexpressing Arabidopsis NAD Kinase Gene. *Plant Physiol.***2010**, *152*, 1863–1873, doi:10.1104/pp.110.153098.
59. Wang, W.-H.; Chen, J.; Liu, T.-W.; Chen, J.; Han, A.-D.; Simon, M.; Dong, X.-J.; He, J.-X.; Zheng, H.-L. Regulation of the Calcium-Sensing Receptor in Both Stomatal Movement and Photosynthetic Electron Transport Is Crucial for Water Use Efficiency and Drought Tolerance in Arabidopsis. *J. Exp. Bot.***2014**, *65*, 223–234, doi:10.1093/jxb/ert362.

Figure Legends

Figure 1. The conservation and diversification of MIR408 family in plants. **(a)** Comparison of MIR408 family expansion in plants. The plot demonstrates the number of plant species with one to multiple MIR408 precursors. **(b)** miR408 (mature) size distribution for 156 MIR408 precursors annotated in 97 plant species. **(c)** Comparative analysis of different miR408 sequence variants (F-1 to F-14) and their frequency across different lineage of plant kingdom. **(d)** Phylogenetic analysis of 156 MIR408 annotated precursors from 97 plant species using MEGA 11 software following Maximum likelihood method and Tamura-

Preprints (www.preprints.org) | NOT PEER-REVIEWED | Posted: 8 February 2022 doi:10.20944/preprints202202.0113.v1

Nel model. The different groups were labeled through GI-VI. The different colored dots highlight the precursors belonging to species with 2 to 6 family members.

Figure 2. Sequence variants and haplotype analysis of MIR408 and its promoter region in 4726 rice accessions. (a) The plots show the position and frequency of primary allele of variants identified in the region of MIR408 and its promoter region (1 kb) using RiceVarMap2 database. The co-ordinates marked with green and red line represents the promoter and precursor of miR408 respectively. **(b)** The detailed list of variants with primary and secondary alleles **(c)** the plot showing the result of haplotype network analysis. Only haplotypes found in ≥10 rice accessions were used to construct the haplotype network. **(d)** The details of eight haplotype detected on the basis of variants in the promoter region.

Figure 3. Transcriptional regulation of miR408 in different tissues of N22 under control and drought stress conditions. (a) miR408-3p expression in flag leaf (FL), inflorescence (INF) and roots (RT) of N22 under control conditions. **(b)** Drought-mediated expression of miR408-3p in root (RT), flag leaf (FL) and inflorescence (INF) of N22. **(c) T**he drought mediated expression levels of pre-MIR408 in flag leaf (FL) and roots (RT) of N22. **(d-e)** The comparison of methylation levels (single base level) of different context i.e. CpG, CHG and CHH in promoter (1kb upstream of pre-MIR408) and precursor region (Ch01: 12301661-12301873) of MIR408 in different tissues of N22 under control and drought conditions. Only the methylation levels following the p-value criterion of ≤ 0.05 were shown in the figure.

Figure 4. Comparison of miR408-3p and its target gene expression in rice. (a) The expression comparison of miR408-3p and its target genes in roots with respect to flag leaf under control conditions. **(b-c)** The drought-mediated comparative expression analysis of miR408-3p/target module in roots (b) and flag leaf (c) of N22. **(d)** qRT-PCR Validation of root-enriched drought responsive miR408-3p targets and pre-MIR408 in roots of N22. The expression was mean of three biological replicates and three technical repeats were used. Rice actin gene was used as the endogenous control. **(e)** The relative expression level of different miR408-3p targets and pre-MIR408 in RNA-seq of transgenic rice seedlings overexpressing MIR408 were demonstrated by box plot (BioProject PRJNA412295). Each dot represents one target gene. **(f)** the upset plot showing the intersection and overlap of miR408-3p targets showing opposite expression to miR408-3p in different conditions in rice.

 doi:10.20944/preprints202202.0113.v1

Figure 5. Effect of MIR408 overexpression on rice growth and photosynthesis. (a-h) Phenotypic comparison of 40 days old wild type and MIR408-OX plants (a-b). Quantitative analysis of shoot (c) and root length (d); root density (e); seedling weight (f); leaf blade width (g), leaf blade length (h) and picture of leaf blade (i). **(j)** Chlorophyll content in the wild type and MIR408 overexpressing plants. **(k-l)** Comparative analysis of chlorophyll fluorescence parameters; Fv/Fm, Y(II) (k) and ETR (l) between wild type and MIR408-OE plants. For all the estimations 10 biological replicates were used. The asterisks indicate a significant difference between the indicated samples calculated by two tailed students t-test (P-value ≤ 0.05 *, ** ≤ 0.01, ***≤ 0.001). **(m)** The qRT-PCR based comparative expression of MIR408 and its target genes in MIR408-OE plants. Rice actin was used as an internal control. For each condition three technical and three biological replicates were analysed. The error bars in graphs denote standard error.

Figure 6. Dehydration response of MIR408-OE plants at seedling stage. (a-f) pictures showing the phenotype of WT and MIR408-OE plants after 0 h, 1 h, 7 h of PEG treatment and recovery. **(g-k)** Estimation of Relative water content (g; $n= 3$) , Fv/Fm (h; $n= 5$), Y(II) (I; $n= 5$), ETR (j; $n= 5$) and seedling weight (k; $n= 5$) after 7 h of dehydration stress. 'n' denotes the number of biological replicates. The asterisks indicate a significant difference between the indicated samples calculated by two tailed students t-test {$P \leq 0.05$ (*), $P \leq 0.005$ (**), $P \leq 0.001$ (***)}.

Supplementary Figures

Figure S1. The phylogenetic conservation of miR408 family in plants. (a) The conservation of miR408 across diverse plant species adapted from database PmiREN. The species highlighted in green have annotated miR408. **(b)** The sequence comparison of annotated miR408 in different plant species (n=97). The differences are highlighted in pink color. The conservation is depicted as bars and consensus logo.

Figure S2. The sequence alignment of MIR408 in plants. The sequence comparison of annotated MIR408 in different plant species using alignment tool of CLC genomics (version 9). The conservation and differences or gaps are highlighted in blue and pink color respectively.

 doi:10.20944/preprints202202.0113.v1

Figure S3. Mapping of variants and cis-elements on MIR408 promoter sequence. The 1kb promoter region showing the position and overlap of variants (highlighted in red color) detected in 4726 rice accessions with the different cis-regulatory elements (highlighted in green color) detected in promoter using New Place database.

Figure S4. The phylogenetic tree showing the conservation of miR408 targets. The degradome identified targets were extracted from PmiREN database for 13 diverse species and analyzed following the PhyML 3.0. The conserved target families were highlighted in different colors.

Figure S5. Gene ontology and pathway enrichment of miR408-3p targets in rice. (a-c) GO enrichment analysis of miR408-3p targets in rice using ShyniGO tool showing the enriched terms belonging to cellular component (a), biological process (b) and molecular function (c). The terms with significant enrichment with P-value ≤ 0.05 were shown**. (d)** The expression of miR408-3p targets in flag leaf, inflorescence and root at heading stage of development. The genes marked with green, black and red dots represents the tissue enrichment ≥ 5 in flag leaf, root and inflorescence. The heat map was generated using the fold-enrichment fold change using clustvis online tool following Euclidean distance and complete linkage with unit variance scaling is applied to rows.

Table S6. The comparative summary of regulation of miR408-3p/target in N22 and MIR408-OE overexpression. The detailed expression correlation of miR408-3p targets under drought in flag leaf and root, expression in root w.r.t. flag leaf and in MIR408-OE seedlings. The category and PARE datasets represents the evidence from degradome. The inverse trend in expression of miR408 and its target transcript was represented by * (strength).

Figure S7. The morphometric characterization of different MIR408-OE-lines in T1 generation. (a) Morphometric comparison of wild type PB1 with four MIR408-OX-lines (1, 3,12 and 16); **(b)** qRT-PCR validation of miR408-3p in different transgenic overexpression lines. 5s is used as the endogenous control and two biological and three technical repeats were analyzed for each line. **(c-e)** Box plots represents the comparison of seedling weight,

 doi:10.20944/preprints202202.0113.v1

Shoot length and Root length of WT and MIR408-OE lines. Each value represents the mean of at least 10 plants.

Table S1. The list of sequences of mature miR408 annotated in plants extracted from PmiREN database.

Table S2. The list of precursor MIR408 in plants extracted from PmiREN database.

Table S3: The list of degradome identified targets obtained from pmiREN database

Preprints (www.preprints.org) | NOT PEER-REVIEWED | Posted: 8 February 2022 doi:10.20944/preprints202202.0113.v1

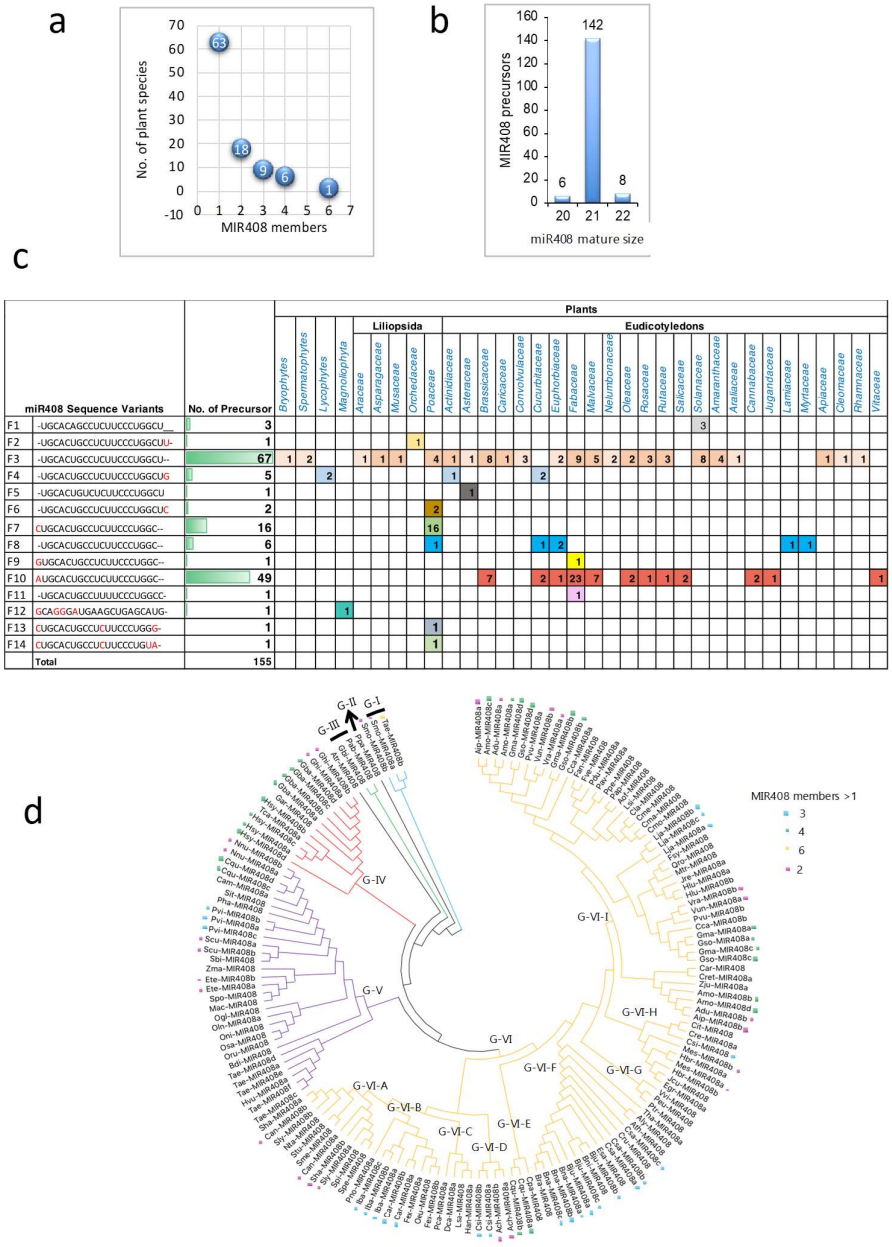

Figure 1. The conservation and diversification of MIR408 family in plants. **(a)** Comparison of MIR408 family expansion in plants. The plot demonstrate the number of plant species with one to multiple MIR408 precursors. **(b)** miR408 (mature) size distribution for 156 MIR408 precursors annotated in 97 plant species. **(c)** Comparative analysis of different miR408 sequence variants (F-1 to F-14) and their frequency across different lineage of plant kingdom. **(d)** Phylogenetic analysis of 156 MIR408 annotated precursors from 97 plant species using MEGA 11 software following Maximum likelihood method and Tamura-Nel model. The different groups were labeled through GI-VI. The different colored dots highlights the precursors belonging to species with 2 to 6 family members.

Preprints (www.preprints.org) | NOT PEER-REVIEWED | Posted: 8 February 2022 doi:10.20944/preprints202202.0113.v1

a

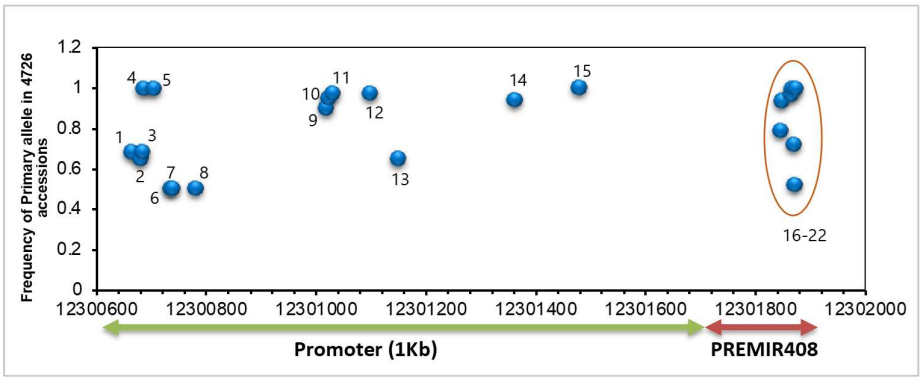

b

S.no.		Var ID	Reference	Primary Allele	Secondary Allele
1	Promoter	vg0112300662	A	G	A
2		vg0112300679	A	G	A
3		vg0112300683	A	G	A
4		vg0112300685	G	G	T
5		vg0112300704	TG	TG	T
6		vg0112300734	C	C	T
7		vg0112300737	AG	AG	A
8		vg0112300779	A	A	C
9		vg0112301017	TTTTA	TTTTA	T
10		vg0112301021	AT	AT	A
11		vg0112301030	T	T	C
12		vg0112301098	AAGT	AAGT	A
13		vg0112301149	CTGCCTTTTTT	C	CTGCCTTTTTT
14		vg0112301361	G	G	C
15		vg0112301478	TA	TA	T
16	Precursor MIR408	vg0112301845	CCTCT	CCTCT	CCTCTCT
17		vg0112301846	CT	CT	C
18		vg0112301864	CTCTCTG	CTCTCTG	C
19		vg0112301866	CTCTGTG	CTCTGTG	CTG
20		vg0112301868	CTGTG	CTGTG	CTG
21		vg0112301870	G	G	C
22		vg0112301872	G	G	C

c

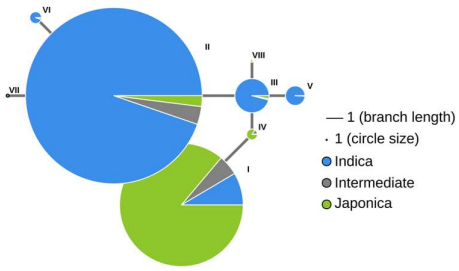

d

Haplotype Group	Haplotype	ALL Frequencies	Indica	Japonica	Intermediate
I	AAAGCATG	1516	129	1306	81
II	GGGGTCTG	2167	2053	43	71
III	GGGGCATG	420	403	12	5
IV	GAGGCATG	133	3	112	18
V	GGGGCATC	240	238	0	2
VI	GGGGTCCG	145	137	1	7
VII	GGGGTCTC	36	36	0	0
VIII	GGGTCATG	38	8	30	0

Figure 2. Sequence variants and haplotype analysis of MIR408 and its promoter region in 4726 rice accessions. (a) The plots shows the position and frequency of primary allele of variants identified in the region of MIR408 and its promoter region (1 kb) using RiceVarMap2 database. The co-ordinates marked with green and red line represents the promoter and precursor of miR408 respectively. **(b)** the detailed list of variants with primary and secondary alleles **(c)** the plot showing the result of haplotype network analysis. Only haplotypes found in ≥10 rice accessions were used to construct the haplotype network. **(d)** the details of eight haplotype detected on the basis of variants in the promoter region.

Preprints (www.preprints.org) | NOT PEER-REVIEWED | Posted: 8 February 2022 doi:10.20944/preprints202202.0113.v1

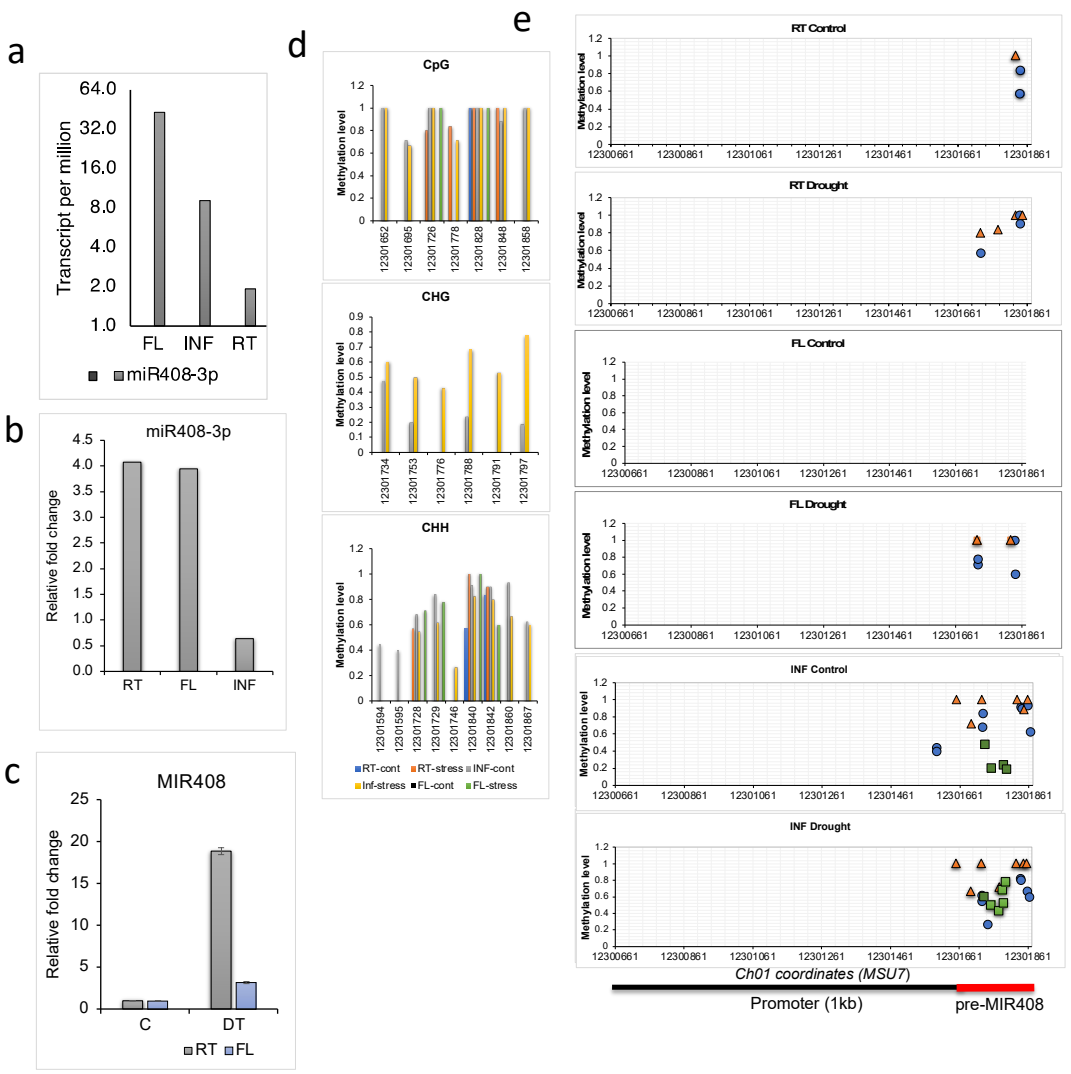

Figure 3. Transcriptional regulation of miR408 in different tissues of N22 under control and drought stress conditions. (a) miR408-3p expression in flag leaf (FL), inflorescence (INF) and roots (RT) of N22 under control conditions. **(b)** Drought-mediated expression of miR408-3p in root (RT), flag leaf (FL) and inflorescence (INF) of N22. **(c) T**he drought mediated expression levels of pre-MIR408 in flag leaf (FL) and roots (RT) of N22. **(d-e)** The comparison of methylation levels (single base level) of different context i.e. CpG, CHG and CHH in promoter (1kb upstream of pre-MIR408) and precursor region (Ch01: 12301661-12301873) of MIR408 in different tissues of N22 under control and drought conditions. Only the methylation levels following the p-value criterion of ≤ 0.05 were shown in the figure.

Preprints (www.preprints.org) | NOT PEER-REVIEWED | Posted: 8 February 2022 doi:10.20944/preprints202202.0113.v1

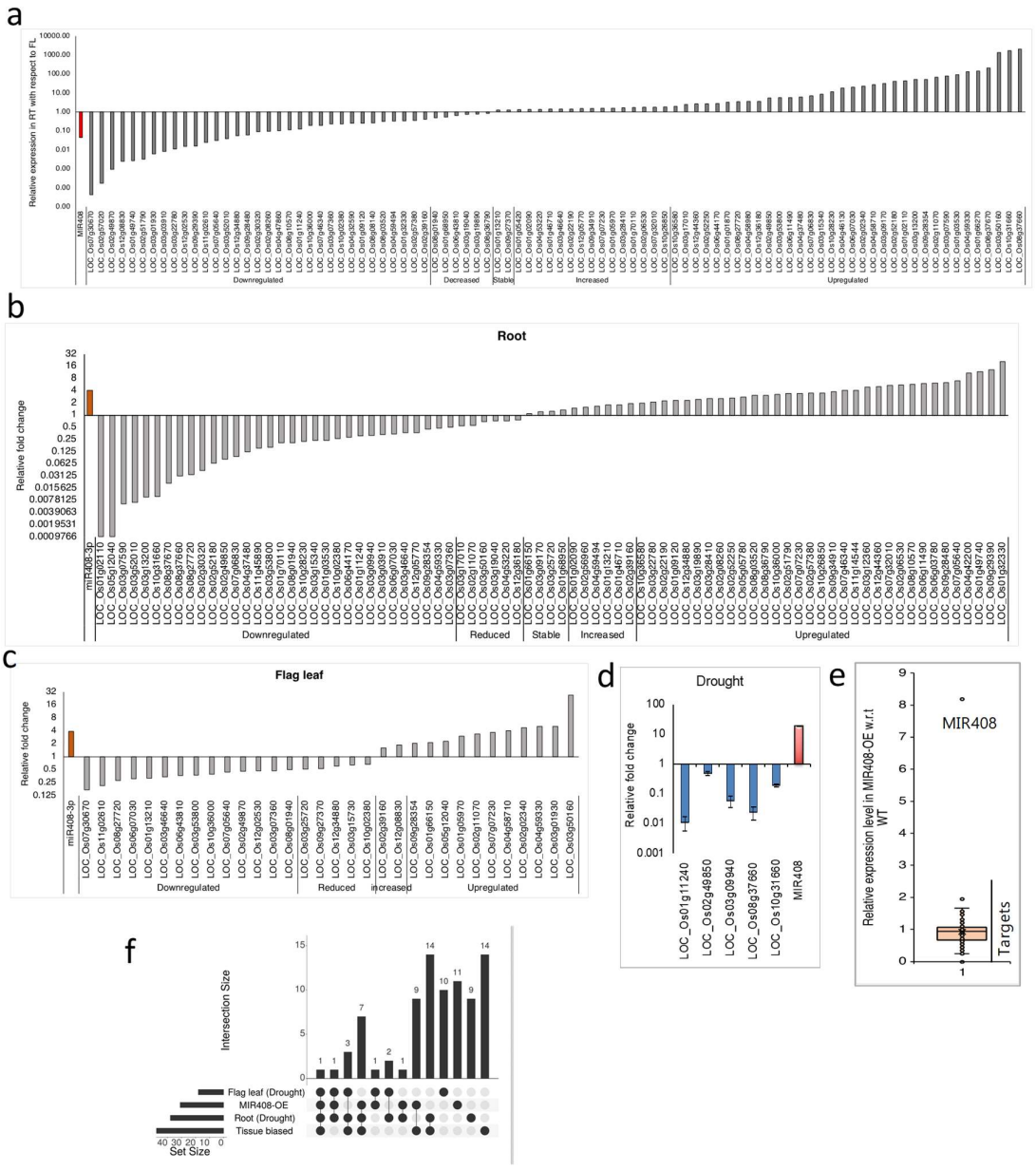

Figure 4. Comparison of miR408-3p and its target gene expression in rice. (a) The expression comparison of miR408-3p and its target genes in roots with respect to flag leaf under control conditions. **(b-c)** The drought-mediated comparative expression analysis of miR408-3p/target module in roots (b) and flag leaf (c) of N22. **(d)** qRT-PCR Validation of root-enriched drought responsive miR408-3p targets and pre-MIR408 in roots of N22. The expression was mean of three biological replicates and three technical repeats were used. Rice actin gene was used as the endogenous control. **(e)** The relative expression level of different miR408-3p targets and pre-MIR408 in RNA-seq of transgenic rice seedlings overexpressing MIR408 were demonstrated by box plot (BioProject PRJNA412295). Each dot represents one target gene. **(f)** the upset plot showing the intersection and overlap of miR408-3p targets showing opposite expression to miR408-3p in different conditions in rice.

Preprints (www.preprints.org) | NOT PEER-REVIEWED | Posted: 8 February 2022 doi:10.20944/preprints202202.0113.v1

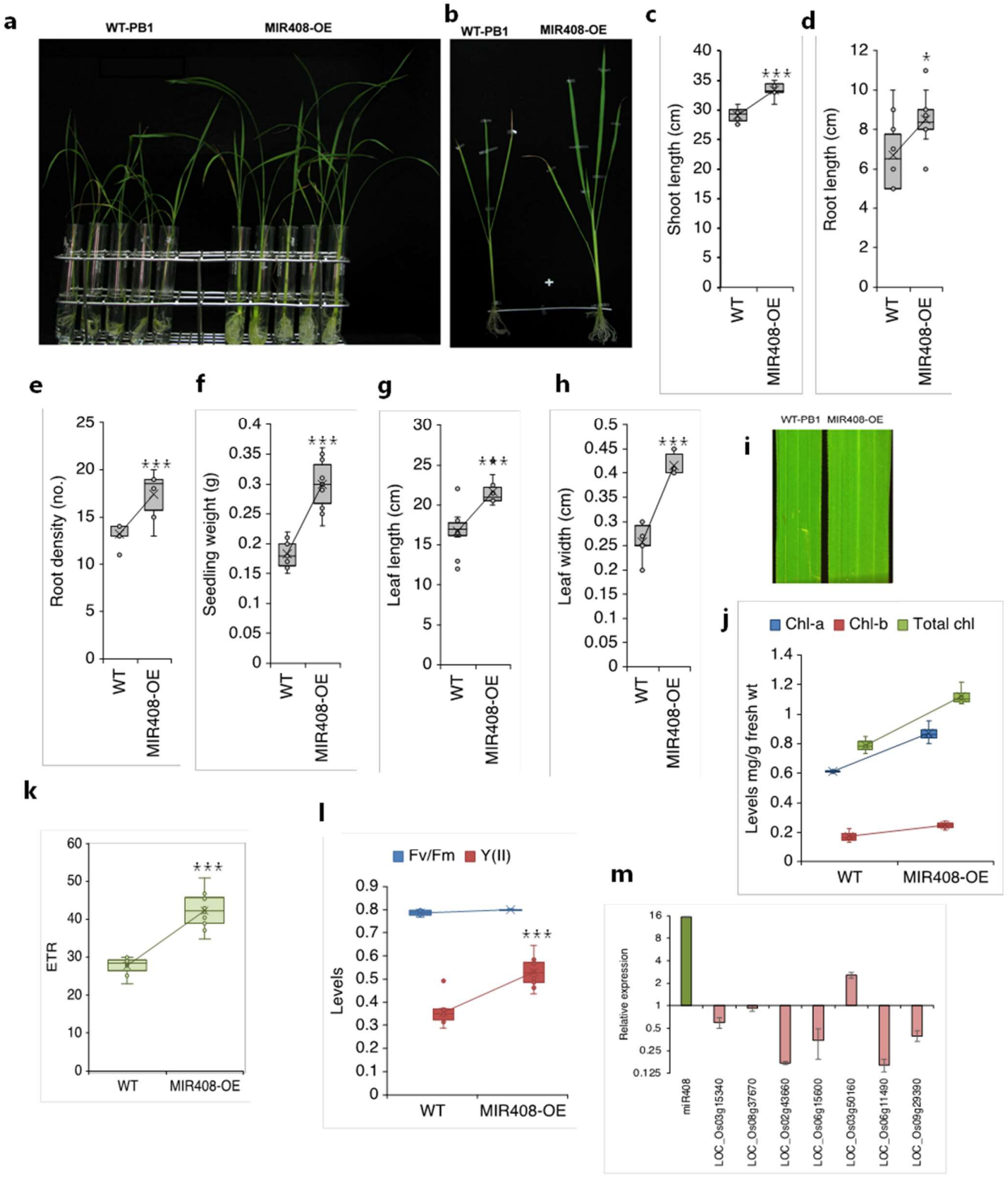

Figure 5. Effect of MIR408 overexpression on rice growth and photosynthesis. (a-h) Phenotypic comparison of 40 days old wild type and MIR408-OX plants (a-b). Quantitative analysis of shoot (c) and root length (d); root density (e); seedling weight (f); leaf blade width (g), leaf blade length (h) and picture of leaf blade (i). **(j)** Chlorophyll content in the wild type and MIR408 overexpressing plants. **(k-l)** Comparative analysis of chlorophyll fluorescence parameters; Fv/Fm, Y(II) (k) and ETR (l) between wild type and MIR408-OE plants. For all the estimations 10 biological replicates were used. The asterisks indicate a significant difference between the indicated samples calculated by two tailed students t-test (P-value ≤ 0.05 *, ** ≤ 0.01, ***≤ 0.001). **(m)** The qRT-PCR based comparative expression of MIR408 and its target genes in MIR408-OE plants. Rice actin was used as an internal control. For each condition three technical and three biological replicates were analysed. The error bars in graphs denote standard error.

Preprints (www.preprints.org) | NOT PEER-REVIEWED | Posted: 8 February 2022 doi:10.20944/preprints202202.0113.v1

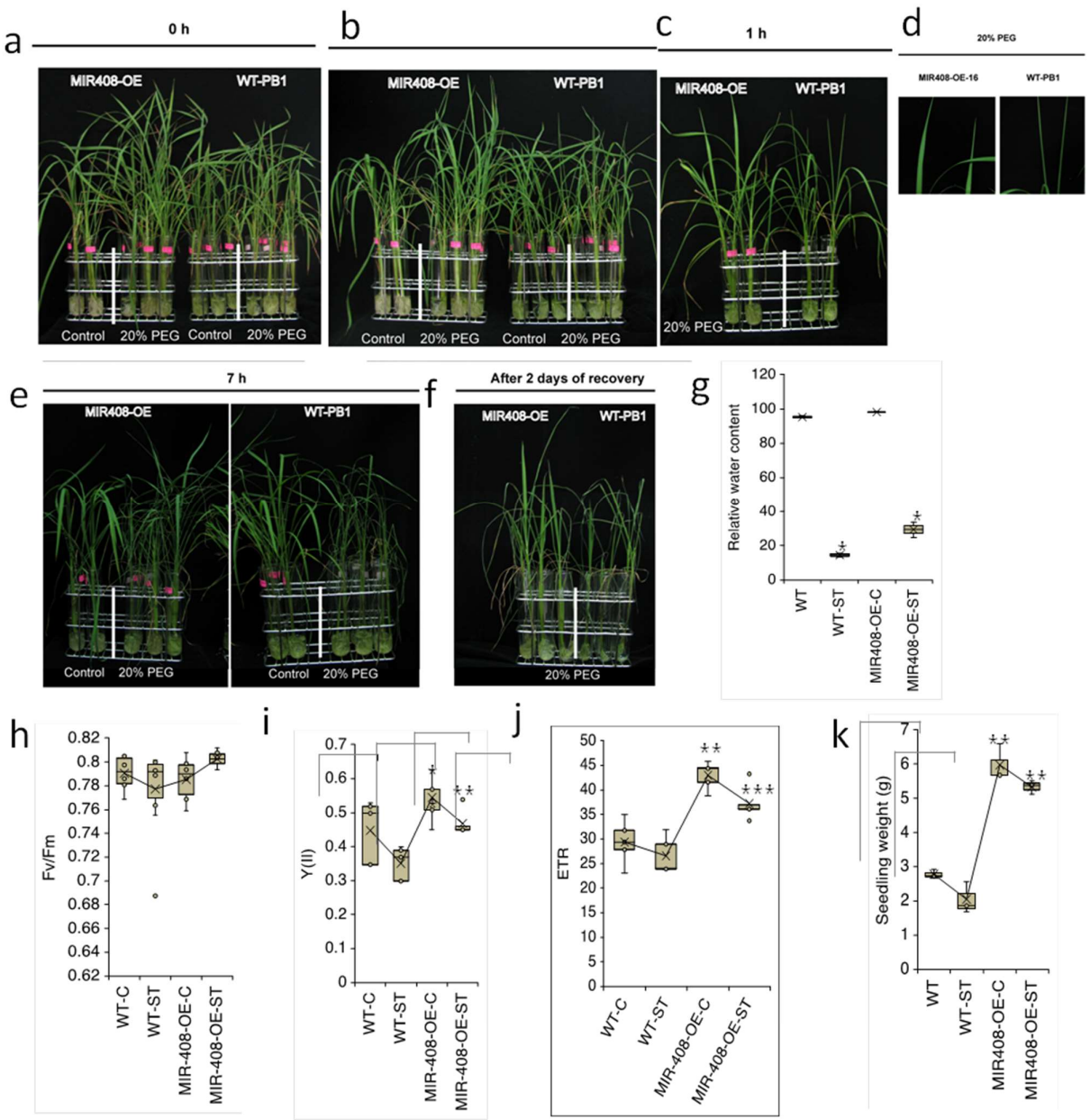

Figure 6. Dehydration response of MIR408-OE plants at seedling stage. (a-f) pictures showing the phenotype of WT and MIR408-OE plants after 0 h, 1 h, 7 h of PEG treatment and recovery. **(g-k) Estimation of** Relative water content (g; *n= 3*) , Fv/Fm (h; *n= 5*), Y(II) (I; *n= 5*), ETR (j; *n= 5*) and seedling weight (k; *n= 5*) after 7 h of dehydration stress. 'n' denotes the number of biological replicates. The asterisks indicate a significant difference between the indicated samples calculated by two tailed students t-test {P ≤ 0.05 (*), P ≤ 0.005 (**), P ≤ 0.001 (***)}.

 doi:10.20944/preprints202202.0113.v1